TABLE 1. Clinical Characteristics of Study Subjects

Characteristic	Nonsmokers		Smokers	
	Female (n = 24)	Male (n = 15)	Male (n = 11)	P*
Age (y)	60±2	63±4	48±4†	.04
Risk factors for coronary artery disease				
Hyperlipidemia	3 (13%)	1 (7%)	0 (0%)	NS
Diabetes mellitus	4 (17%)	4 (27%)	1 (9%)	NS
Hypertension	18 (75%)	8 (53%)	3 (27%)	.03
Family history	3 (13%)	3 (20%)	1 (9%)	NS
Medication				
Aspirin	3 (13%)	2 (13%)	2 (18%)	NS
Statins	4 (17%)	1 (7%)	0 (0%)	NS
ACE inhibitors	3 (13%)	3 (20%)	2 (18%)	NS
Antioxidants	1 (4%)	1 (7%)	1 (9%)	NS

Data presented are mean value ± SEM or number (%) of patients.

*Kruskal-Wallis test (for continuous values) and Fisher's exact test (for discrete variables) were used to compare the values across the three groups.

†Significantly different from male nonsmokers by Mann-Whitney *U* test.

NS = Not significant; ACE = angiotensin converting enzyme.

Oligonucleotide Primers and Probes

The oligonucleotide sequences used for primers and as hybridization probes for the target are shown in Fig. 1. eNOS primers and probes were designed using the Primer Express V1.0 program, Applied Biosystems Division, Perkin-Elmer (Foster City, CA, USA). The forward and reverse primers specific for human eNOS were designed to span the region within exon 11 to 12 where the nucleotide sequence was not conserved among the three NOS isoforms. The eNOS target probe was designed to span an exon/intron junction to avoid hybridization with genomic DNA sequences. The target (eNOS) and the internal control (GAPDH) probes were labeled with reporter dye FAM (6-carboxyfluorescein) and JOE (6-carboxy-4,5-dichloro-2,7-dimethoxyfluorescein) at the 5' ends, respectively. Both probes were labeled with the quencher fluor TAMRA (6-carboxy-tetramethylrhodamine) at the 3' end followed by the phosphorylation site P.

Oligo-nucleotide hybridization probes were obtained from Applied Biosystems Division, Perkin-Elmer and primers were obtained from SAWADAY, Inc. (Tokyo, Japan).

Real-time QC RT-PCR Analysis

We prepared 200 ng of total RNA sample in each tube, and determined the relative copy numbers of eNOS mRNA and GAPDH mRNA in human platelets (as a target and an internal control) by the sensitive method of real-time RT-PCR (PRISM™ 7700 Sequence Detector, Applied Biosystems Division, Perkin-Elmer). In every assay, we also measured both eNOS and GAPDH mRNA copy numbers in cultured human aortic endothelial cells which were then used to derive a standard curve for RT-PCR analysis. The principle of real-time RT-PCR detection is based on the fluorogenic 5' nuclease assay as described earlier (23). Briefly, following reverse transcription, the nucleolytic activity of the rTth DNA polymerase will cleave an oligonucleotide probe hybridized to the target cDNA during the PCR reaction. The fluorescent reporters FAM and JOE located on the 5' ends of the probe molecules are released from a quencher dye TAMRA present on the 3' end. Fluorescent emission is measured in real-time and threshold cycles (CT) are calculated, which reflect the starting mRNA quantities (Fig. 2). These data were analyzed with a Sequence Detector V1.6 program, Perkin-Elmer.

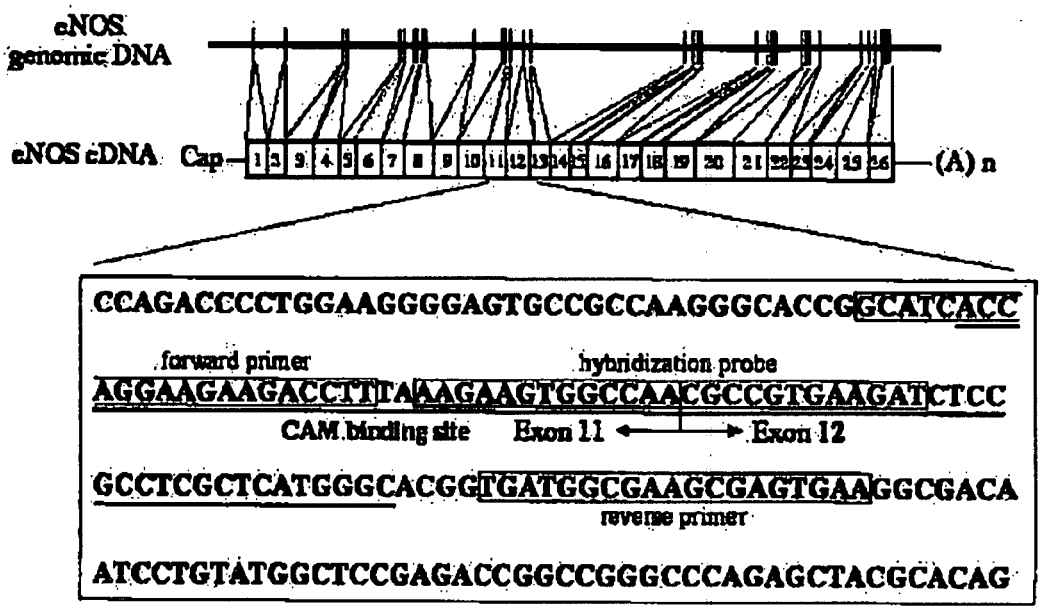

FIG. 1. Nucleotide sequence of human endothelial NOS (eNOS) utilized for PCR-amplification of intraplatelet eNOS cDNA. Forward and reverse primers and hybridization probe specific for human eNOS are shown in the boxes. CAM binding site is noted by the underline.

Statistical Analysis

All data are expressed as mean±SEM. The clinical data were compared using the Kruskal Wallis test and Mann-Whitney *U* test (for continuous values), and Fisher's exact test (for discrete variables). We used multivariate linear regression analysis for the whole study population to determine which clinical characteristics were significantly associated with platelet eNOS mRNA expression levels. Statistical significance was accepted at a *P* value less than .05. All analyses were undertaken using the Statistical Package for Social Scientists 6.1 software, SPSS Japan Inc. (Tokyo, Japan).

RESULTS

Characteristics of Study Subjects

The mean cigarette exposure in smokers (all male) was 19±3 cigarettes per day for 28±4 years. As shown in Table 1, there were several minor differences in baseline characteristics (age and hypertension) among the three groups. The drug administration of aspirin, statins, angiotensin converting enzyme inhibitors, and antioxidant (vitamin E) did not differ among the three groups.

Intra-assay and Interassay Precision

Single bands of 91 bp (target) and 226 bp (internal control) could be detected by gel electrophoresis in the RT-PCR products of all samples, and each length conformed to the expected size of the RT-PCR products of eNOS and GAPDH mRNA. The correspondence of the sequences between the amplified intraplatelet NOS and endothelial NOS indicates that eNOS mRNA expression was identified in human platelets.

As shown in Fig. 2A and 2B, both eNOS and GAPDH mRNA are reverse transcribed, detected, and quantitated in real-time. Total RNA from cultured human aortic endothelial cells was used to derive standard curves for both eNOS and GAPDH mRNA in every assay. The linearity of eNOS and GAPDH mRNA detection was tested using serially diluted total RNA (0.02 to 4 ng/μL) from cultured human aortic endothelial cells in every assay. Using this specific protocol, the assay shows very good linearity within this range (correlation coefficient, $r > 0.95$). The linearity of the detection allowed a simple calculation of sample eNOS and GAPDH contents by using linear regression analysis (bottom in Fig. 2). To determine intra-assay and inter-assay precision, triplicate sets of known concentration (2000 relative copies) of eNOS and GAPDH mRNA were

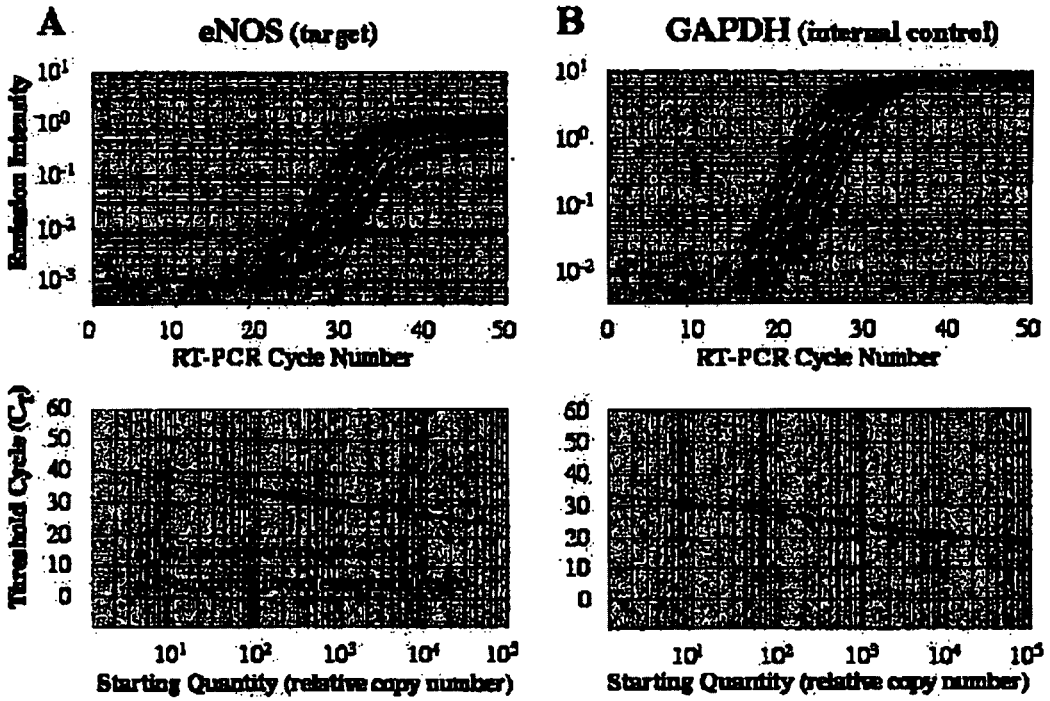

FIG. 2. Representative amplification plots (top) and standard curves (bottom) of the real-time quantitative reverse transcriptase polymerase chain reaction (QC RT-PCR) method. A: Measurement of endothelial nitric oxide synthase (eNOS) mRNA in human platelets (unknowns) and human aortic endothelial cells (standards). B: Measurement of glyceraldehyde-3-phosphate dehydrogenase (GAPDH) mRNA in both samples.

reverse transcribed and amplified in every assay at the same time of other unknown sets. The intra-assay and inter-assay variation were found to be 8±2% and 11±3% in eNOS mRNA levels normalized to GAPDH mRNA levels.

Quantitation of Intraplatelet eNOS mRNA Expression Levels

As shown in Fig. 3, there was significant expression of eNOS mRNA in platelets from each group. In a comparison between smokers and nonsmokers, the expression level of eNOS mRNA (relative copy number) was found to be significantly lower in male smokers (59±17) than in male and female nonsmokers (195±71 and 285±60, $P = .02$ and $P < .0001$, respectively). In a comparison between males and females, the level of eNOS mRNA was significantly higher in female nonsmokers (285±60) than in male nonsmokers (195±71, $P < .03$). In a comparison between premenopausal (n = 5; 23 to 50 years of age) and postmenopausal (n = 19; 53 to 79 years of age) women, there was a tendency of higher expression level in premenopausal women (481±231) than in postmenopausal women (234±43, P = ns).

Multivariate Analysis of eNOS mRNA Expression Levels

Table 2 shows the result of multiple linear regression analysis on the eNOS mRNA expression level and other clinical variables. In all subjects, cigarette smoking ($P = .008$) and diabetes mellitus ($P = .047$) were found to be significantly negative predictors, and antioxidant (vitamin E) treatment ($P = .01$) was a significantly positive predictor of platelet eNOS mRNA expression. Age, other medications, and other risk factors for coronary artery disease were not significant.

DISCUSSION

This study is the first to demonstrate the quantitation of eNOS mRNA expression levels in human platelets. We applied a quantitative RT-

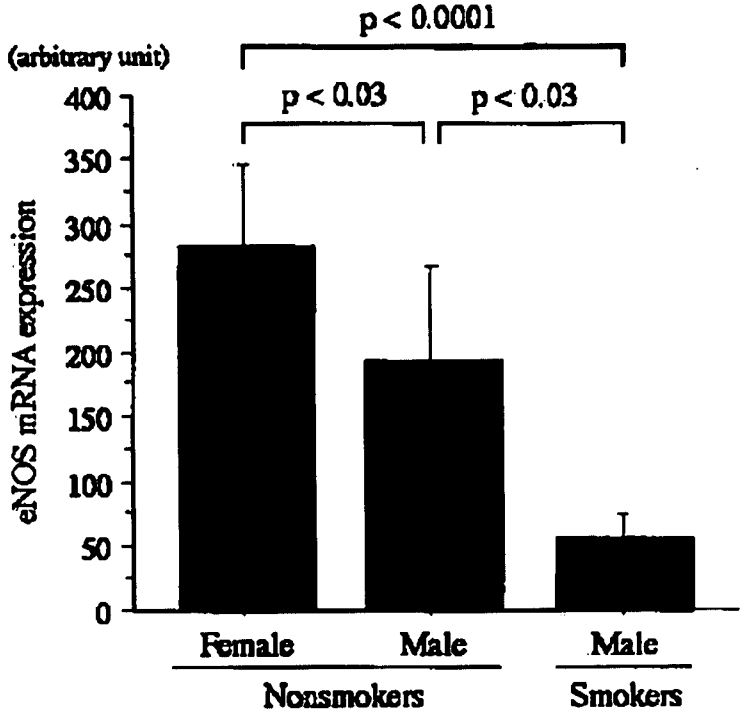

FIG. 3. The relative value of endothelial nitric oxide synthase (eNOS) mRNA levels normalized to glyceraldehyde-3-phosphate dehydroganase (GAPDH) mRNA levels. Values are the means ± ?SEM.

TABLE 2. Multivariate Linear Regression Analysis for Factors Potentially Linked to eNOS mRNA Expression Level

Variable	B	SE(B)	Beta	*t*	*P*
Cigarette smoking	-229.7	82.78	-0.3629	-2.775	.008
Antioxidant treatment	405.1	151.25	0.3668	2.678	.010
Diabetes mellitus	-191.8	93.99	-0.2810	-2.041	.047
(Constant)	269.2	42.40		6.349	.000

Final significant variables in the equation by stepwise selection method.
B: Partial regression coefficients; SE (B): standard errors of the coefficients; Beta: standardized partial regression coefficients, *P*: two-tailed probability of *t*.

PCR method, using fluorescent hybridization probes and a sequence detector. We measured individual expression levels of eNOS gene by collecting blood samples and using this method as a bioassay. We also showed that platelet eNOS mRNA expression levels were significantly decreased in cigarette smokers by using univariate and multivariate analyses.

The quantitation of platelet eNOS mRNA expression is based on a recently developed method. The direct study of platelet-specific gene products has been greatly hampered, because human platelets are derived from megakaryocytes as a-nucleate cells and contain only trace amounts of RNA capable of being transcribed into protein. We used a quantitative real-time RT-PCR technique based on the sensitive fluorescence detection system to make these quantitations. The amount of total RNA necessary for assay was much less than that of Northern blot and RNase protection analyses. In addition, this method allowed for the detection and quantitation of low abundance target molecules with high accuracy.

During the last few years, evidence has been accumulating to suggest that platelets themselves have an L-arginine/NO pathway that may act as a negative feedback mechanism to inhibit excessive adhesion, secretion, and aggregation of platelets (7,8). Under resting conditions, the source of NO acting on platelets is most likely the endothelium. But under conditions associated with disrupted, diseased endothelium and platelet activation, platelet-derived NO appears to play an important counterregulatory role by inhibiting recruitment of platelets to the growing thrombus (8). Recently, constitutive NOS has been identified in human blood platelets and revealed to be endothelial NOS in origin (5,6). To quantitate platelet NOS mRNA accurately, it is necessary to develop an eNOS mRNA detection method which does not cross-react with other NOS mRNAs. In our assay, no cross-reactivity with the other NOS mRNA (nNOS mRNA or iNOS mRNA) was observed because of the specific design of the oligo-nucleotide hybridization probes and primers.

It has recently been reported that platelet-derived NO release is impaired in long-term smokers (17) and patients with acute coronary syndrome (ACS) (24), but the mechanism(s) for decreased NO release from platelets in those subjects have not yet been established. The present study showed that intraplatelet eNOS mRNA expression is significantly decreased in cigarette smokers. The reduced expression of intraplatelet eNOS mRNA in smokers may play an important role in the pathogenesis of ACS, such as unstable angina pectoris and myocardial infarction.

In this study, the expression level of platelet eNOS mRNA was associated with gender difference (female nonsmokers vs male nonsmokers), as was difference of smoking status (male smokers vs male nonsmokers). Higher expression level of platelet eNOS mRNA in female subjects may suggest that estrogen could upregulate eNOS gene expression in platelets, as in endothelial cells (25,26). In the analysis of female subjects, the expression level tends to be higher in premenopausal women than in postmenopausal women, but did not reach statistical significance. In recent studies, nongenomic effect of estrogen on eNOS cellular targeting (27) and other estrogen-regulated genes such as prostacyclin synthase have been reported. Estrogen may have other main effects on premenopausal women, rather than enhancement of eNOS mRNA expression.

Multiple linear regression analysis showed that cigarette smoking, antioxidant (vitamin E) treatment, and diabetes mellitus were significant predictors of platelet eNOS mRNA expression level. These final significant risk factors and medication may all alter intraplatelet and -megakaryocyte redox status (28,29). Oxidatively modified LDL regulates eNOS expression through a combination of early transcriptional inhibition and posttranscriptional mRNA destabilization in human endothelial cells (30), and also decreases eNOS protein expression in human platelets (31). Exposure to cigarette smoke might modify directly or indirectly the rate of transcription of eNOS gene and/or the stability of the transcripts because of its association with the free radical induction of oxidative stress.

Both an increase and a decrease of eNOS mRNA and protein have been found in endothelial cells treated with cigarette smoke extract and nicotine (32,33). The present study is the first to demonstrate that long-term cigarette smoking reduces platelet eNOS mRNA expression that could lead to decreased eNOS protein mass in human platelets. We speculate that oxidative stress by long-term smoking results in down-regulation of platelet eNOS gene directly or indirectly (transcriptional inhibition and/or posttranscriptional mRNA destabilization) more than up-regulation based on a feedback mechanism thought to be triggered by reduced eNOS activity and NO breakdown.

We previously showed that an eNOS gene mutation in the promoter region (T-786 to C) reduces gene promoter activity (34,35). It will be interesting to explore the differences in intraplatelet eNOS mRNA expression levels between carriers and noncarriers of this gene mutation. Given that the effects of this eNOS gene mutation and low expression of the eNOS gene caused

by long-term smoking could potentially be additive, subjects carrying this genetic trait should be strongly cautioned against cigarette smoking. Demonstration of an additive effect requires confirmation by future studies.

Study Limitations

A total of 50 subjects enrolled in this study included no female smokers, although they were consecutive subjects who had been referred to our hospital and had given informed consent to the study. We can assume that this bias is excluded by the result of multivariate analysis; sex difference was not a significant predictor of platelet eNOS mRNA expression level. However, it may have led us to underestimate the effect of sex difference on eNOS mRNA expression levels.

We had to collect large amounts of whole blood (40 mL) from each subject, because human platelets contain only trace amounts of RNA. We adapted the acid-guanidinium-phenol-chloroform extraction procedure and recovered sufficient platelet RNA (approx. 10 to 30 μg of total RNA) to perform QC RT-PCR analysis on platelet eNOS mRNA. Northern blot or RNase protection analyses, however, would require the collection of even greater amounts of whole blood than the QC RT-PCR analysis.

CONCLUSIONS

In this study, we developed a sensitive and accurate quantitative RT-PCR method for measurement of individual expression levels of platelet-derived NOS mRNA. Using this method, we demonstrated that platelet-derived NOS mRNA expression is decreased in smokers compared to nonsmokers. This finding may indicate a pathophysiological link between cigarette smoking and cardiovascular thrombosis, and contribute to the understanding of the high risk of cardiovascular disease in cigarette smokers.

REFERENCES

1. Moncada S, Higgs A. The L-arginine—nitric oxide pathway. *N Engl J Med* 1993;329:2002.
2. Loscalzo J, Welch G. Nitric oxide and its role in the cardiovascular system. *Prog Cardiovasc Dis* 1995;38:87.
3. Voetsch B, Jin RC, Loscalzo J. Nitric oxide insufficiency and atherothrombosis. *Histochem Cell Biol* 2004;122:353.
4. Forstermann U, Boissel JP, Kleinert H. Expressional control of the 'constitutive' isoforms of nitric oxide synthase (NOS I and NOS III). *FASEB J* 1998;12:773.
5. Sase K, Michel T. Expression of constitutive endothelial nitric oxide synthase in human blood platelets. *Life Sci* 1995;57:2049.
6. Wallerath T, Gath I, Aulitzky WE, et al. Identification of the NO synthase isoforms expressed in human neutrophil granulocytes, megakaryocytes and platelets. *Thromb Haemost* 1997;77:163.
7. Radomski MW, Palmer RMJ, Moncada S. An L-arginine/nitric oxide pathway present in human platelets regulates aggregation. *Proc Natl Acad Sci USA* 1990;87:5193.
8. Freedman JE, Loscalzo J, Barnard MR, et al. Nitric oxide released from activated platelets inhibits platelet recruitment. *J Clin Invest* 1997;100:350.
9. Loscalzo J. Nitric oxide insufficiency, platelet activation, and arterial thrombosis. *Circ Res* 2001;88:756.
10. Doeber TR. *The Framingham Study: The Epidemiology of Atherosclerotic Disease*. Cambridge, MA: Harvard University Press; 1980:172.
11. McBride PE. The health consequences of smoking. Cardiovascular diseases. *Med Clin North Am* 1992;76:333.
12. Caralis DG, Deligonul U, Kern MJ, et al. Smoking is a risk factor for coronary spasm in young women. *Circulation* 1992;85:905.
13. Yasue H, Kugiyama K. Coronary spasm: Clinical features and pathogenesis. *Int Med* 1997;36:760.
14. Miyamoto S, Ogawa H, Soejima H, et al. Formation of platelet aggregates after attacks of coronary spastic angina pectoris. *Am J Cardiol* 2000;85:494.
15. Celermajer DS, Sorensen KE, Georgakopoulos D, et al. Cigarette smoking is associated with dose-related and potentially reversible impairment of endothelium-dependent dilation in healthy young adults. *Circulation* 1993; 88:2149.
16. Zeiher AM, Schächinger V. Minners J. Long-term cigarette smoking impairs endothelium-dependent coronary arterial vasodilator function. *Circulation* 1995;92:1094.
17. Ichiki K, Ikeda H, Haramaki N, et al. Long-term smoking impairs platelet-derived nitric oxide release. *Circulation* 1996;94:3109.
18. Morrow JD, Frai B, Lonmire AW, et al. Increase in circulating products of lipid peroxidation (F2-isoprostanes) in smokers: Smoking as a cause of oxidative damage. *N Engl J Med* 1995;332:1198.
19. Steinberg D, Parthasarathy S, Carew TE, et al. Beyond cholesterol: Modifications of low-density lipoprotein that increase its atherogenicity. *N Engl J Med* 1989;320:915.
20. Nakayama T, Kaneko M, Kodama M, et al. Cigarette smoke induces DNA single strand breaks in human cells. *Nature (Lond)* 1985;314:462.
21. Murohara T, Kugiyama K, Ohgushi M, et al. Cigarette smoke extract contracts isolated porcine coronary arteries by superoxide anion-mediated degradation of EDRF. *Am J Physiol* 1994;266:H874.
22. Chomczynski P, Sacchi N. Single-step method of RNA isolation by acid guanidinium thiocyanate-phenol-chloroform extraction. *Anal Biochem* 1987;162:156.
23. Gibson UEM, Heid CA, Williams PM. A novel method for real time quantitative RT-PCR. *Genome Res* 1996;6:995.
24. Freedman JE, Ting B, Hankin B, et al. Impaired platelet production of nitric oxide predicts presence of acute coronary syndromes. *Circulation* 1998;98:1481.

25. Weiner CP, Lizasoain I, Baylis SA, et al. Induction of calcium-dependent nitric oxide synthases by sex hormones. *Proc Natl Acad Sci USA* 1994;91:5212.

26. MacRitchie AN, Jun SS, Chen Z, et al. Estrogen upregulates endothelial nitric oxide synthase gene expression in fetal pulmonary endothelium. *Circ Res* 1997;81:355.

27. Goetz RM, Thatte HS, Prabhakar P, et al. Estradiol induces the calcium-dependent translocation of endothelial nitric oxide synthase. *Proc Natl Acad Sci USA* 1999;96:2788.

28. Mazzanti L, Mutus B. Diabetes-induced alterations in platelet metabolism. *Clin Biochem* 1997;30:509.

29. Baynes JW, Thorpe SR. Role of oxidative stress in diabetic complications: A new perspective on an old paradigm. *Diabetes* 1999;48:1.

30. Liao JK, Shin WS, Lee WY, et al. Oxidized low-density lipoprotein decreases the expression of endothelial nitric oxide synthase. *J Biol Chem* 1995;270:319.

31. Chen LY, Mehta P, Mehta JL. Oxidized LDL decreases L-arginine uptake and nitric oxide synthase protein expression in human platelets. *Circulation* 1996;93:1740.

32. Barua RS, Ambrose JA, Reynolds LJE, et al. Dysfunctional endothelial nitric oxide biosynthesis in healthy smokers with impaired endothelium-dependent vasodilatation. *Circulation* 2001;104:1905.

33. Su Y, Han W, Giraldo C, et al. Effect of cigarette smoke extract on nitric oxide synthase in pulmonary artery endothelial cells. *Am J Respir Cell Mol Biol* 1998;19:819.

34. Nakayama M, Yasue H, Yoshimura M, et al. T-786 C mutation in the 5'-flanking region of the endothelial nitric oxide synthase gene is associated with coronary spasm. *Circulation* 1999;99:2864.

35. Miyamoto Y, Saito Y, Nakayama M, et al. Replication protein A1 reduces transcription of the endothelial nitric oxide synthase gene containing a T-786C mutation associated with coronary spastic angina. *Hum Mol Genet* 2000;9:2629.

THE JOURNAL OF BIOLOGICAL CHEMISTRY VOL. 282, NO. 35, pp. 25445–25452, August 31, 2007

Role of MAPK Phosphatase-1 in the Induction of Monocyte Chemoattractant Protein-1 during the Course of Adipocyte Hypertrophy*[S]

Received for publication, February 21, 2007, and in revised form, June 14, 2007 Published, JBC Papers in Press, July 3, 2007, DOI 10.1074/jbc.M701549200

Ayaka Ito[‡§1], Takayoshi Suganami[‡], Yoshihiro Miyamoto[¶], Yasunao Yoshimasa[¶], Motohiro Takeya[‖], Yasutomi Kamei[‡], and Yoshihiro Ogawa[‡§2]

From the [‡]Department of Molecular Medicine and Metabolism and the [§]Center of Excellence Program for Frontier Research on Molecular Destruction and Reconstitution of Tooth and Bone, Medical Research Institute, Tokyo Medical and Dental University, 2-3-10 Kanda-surugadai, Chiyoda-ku, Tokyo 101-0062, Japan, the [¶]Department of Medicine, Division of Atherosclerosis and Diabetes, National Cardiovascular Center Hospital, 5-7-1 Fujishirodai, Suita, Osaka 560-0005, Japan, and the [‖]Department of Cell Pathology, Graduate School of Medical Sciences, Kumamoto University, 1-1-1 Honjo, Kumamoto 860-8556, Japan

Monocyte chemoattractant protein-1 (MCP-1), an important chemokine whose expression is increased during the course of obesity, plays a role in macrophage infiltration into obese adipose tissue. This study was designed to elucidate the role of mitogen-activated protein kinase (MAPK) phosphatase-1 (MKP-1) in the induction of MCP-1 during the course of adipocyte hypertrophy. We examined the time course of MKP-1 and MCP-1 mRNA expression and extracellular signal-regulated kinase (ERK) phosphorylation in the adipose tissue from mice rendered mildly obese by a short term high fat diet. We also studied the role of MKP-1 in the induction of MCP-1 in 3T3-L1 adipocytes during the course of adipocyte hypertrophy. MCP-1 mRNA expression was increased, followed by ERK activation and down-regulation of MKP-1, an inducible dual specificity phosphatase to inactivate ERK, in the adipose tissue at the early stage of obesity induced by a short term high fat diet, when macrophages are not infiltrated. Down-regulation of MKP-1 preceded ERK activation and increased production of MCP-1 in 3T3-L1 adipocytes *in vitro* during the course of adipocyte hypertrophy. Adenovirus-mediated restoration of MKP-1 in hypertrophied 3T3-L1 adipocytes reduced the otherwise increased ERK phosphorylation, thereby leading to the significant reduction of MCP-1 mRNA expression. This study provides evidence that the down-regulation of MKP-1 is critical for increased production of MCP-1 during the course of adipocyte hypertrophy.

Evidence has accumulated suggesting that obesity is a state of chronic, low grade inflammation; it may represent a potential mechanism whereby obesity leads to the metabolic derangements (1–3). Previous studies demonstrated that the adipose tissue is markedly infiltrated by macrophages in several models of rodent obesities and human obese subjects (4, 5). Using an *in vitro* co-culture system composed of adipocytes and macrophages, we have provided evidence that a paracrine loop involving saturated free fatty acids (FFAs) and tumor necrosis factor-α (TNFα) derived from adipocytes and macrophages, respectively, establishes a vicious cycle that aggravates the inflammatory changes; *i.e.* marked up-regulation of pro-inflammatory cytokines such as monocyte chemoattractant protein-1 (MCP-1)[3] and TNFα and down-regulation of anti-inflammatory adiponectin (6, 7). These findings have led us to speculate that macrophages, when infiltrated, may participate in the inflammatory pathways that are activated in obese adipose tissue.

A previous study with bone marrow transplantation demonstrated that most macrophages in the adipose tissue are derived from the bone marrow (4). In this regard, adipose tissue expression of MCP-1, a major chemokine implicated in the control of monocyte recruitment to the site of inflammation, is increased during the progression of obesity (8, 9) and is roughly correlated with macrophage markers in the adipose tissue (5, 10). These findings suggest that increased production of MCP-1 may be an initial event at the early stage of obesity so as to accumulate macrophages in the adipose tissue. Recently, Kanda *et al.* and Kamei *et al.* (11, 12) have independently reported that MCP-1 plays a role in the recruitment of macrophages into obese adipose tissue. It is, therefore, important to know the molecular mechanism for increased production of MCP-1 at the early stage of obesity. Recent studies have demonstrated that multiple intracellular signaling pathways are activated in adipocytes during the

* This work was supported in part by a grant-in-aid for Scientific Research from the Ministry of Education, Culture, Sports, Science and Technology of Japan, and Ministry of Health, Labor, and Welfare of Japan, and research grants from the Astellas Foundation for Research on Metabolic Disorders, Astellas Foundation for Research on Medicinal Resources and The Ichiro Kanehara Foundation. The costs of publication of this article were defrayed in part by the payment of page charges. This article must therefore be hereby marked "*advertisement*" in accordance with 18 U.S.C. Section 1734 solely to indicate this fact.

[S] The on-line version of this article (available at http://www.jbc.org) contains supplemental Table S1 and Figs. S1–S5.

[1] Supported by the Tokyo Biochemical Research Foundation.

[2] To whom correspondence should be addressed: Dept. of Molecular Medicine and Metabolism, Medical Research Institute, Tokyo Medical and Dental University, 2-3-10 Kanda-surugadai, Chiyoda-ku, Tokyo 101-0062, Japan. Tel.: 81-3-5280-8108; Fax: 81-3-5280-8108; E-mail: ogawa.mmm@mri.tmd.ac.jp.

[3] The abbreviations used are: MCP-1, monocyte chemoattractant protein-1; MAPK, mitogen-activated protein kinase; MKP-1, mitogen-activated protein kinase phosphatase-1; ERK, extracellular signal-regulated kinase; JNK, c-Jun NH_2-terminal kinase; MEK, MAPK/ERK kinase; CAR, coxsackie-adenovirus receptor; WAT, white adipose tissue; GFP, green fluorescent protein; ER, endoplasmic reticulum; ROS, reactive oxygen species; SD, standard diet; HFD, high fat diet; IL, interleukin.

course of adipocyte hypertrophy *in vitro* and in obese adipose tissue *in vivo*. However, how the inflammatory pathways are activated in adipocytes at the early stage of obesity is still poorly understood.

Mitogen-activated protein kinases (MAPKs) including extracellular signal-regulated kinase (ERK), p38 MAPK, and c-Jun NH_2-terminal kinase (JNK) are activated in a variety of cellular processes (13). Once activated by the upstream kinases, *e.g.* MAPK/ERK kinase (MEK), MAPKs are rapidly inactivated by a family of protein phosphatases such as MAPK phosphatase-1 (MKP-1), an inducible dual specificity phosphatase (14, 15). Sakaue *et al.* showed previously that MKP-1 plays an essential role in 3T3-L1 adipocyte differentiation through ERK down-regulation (16). On the other hand, Bost *et al.* (17) reported that mice lacking ERK1 ($ERK1^{-/-}$ mice) are protected from high fat diet-induced obesity and insulin resistance. These findings, taken together, suggest that the MAPK pathways play an important role in the adipocyte proliferation and differentiation *in vitro* and *in vivo* (18).

Here we show that MCP-1 mRNA expression is increased, which is followed by ERK activation and MKP-1 down-regulation in the adipose tissue from mice rendered mildly obese by a short term high fat diet, when macrophages are not infiltrated. We also demonstrate that ERK activation through MKP-1 down-regulation is involved in increased production of MCP-1 in 3T3-L1 adipocytes during the course of adipocyte hypertrophy. This study provides evidence that MKP-1 down-regulation is critical for the inflammatory changes in hypertrophied adipocytes at the early stage of obesity, thereby suggesting that MKP-1 activation may offer a novel therapeutic strategy to treat or reduce the inflammatory changes in adipocytes during the progression of obesity.

EXPERIMENTAL PROCEDURES

Materials—Rabbit polyclonal antibodies against ERK, phospho-ERK, p38 MAPK, phospho-p38 MAPK, MEK1/2, phospho-MEK1/2, MEK inhibitors PD98059 and U0126, and a p38MAPK inhibitor SB203580 were purchased from Cell Signaling (Beverly, MA). Rabbit polyclonal antibodies against JNK, phospho-JNK, and MKP-1 and a mouse monoclonal antibody against Lamin A/C were purchased from Santa Cruz Biotechnology (Santa Cruz, CA). All other reagents were purchased from Sigma or Nacalai Tesque (Kyoto, Japan).

Animal Studies—Four-week-old male C57BL/6J mice were purchased from Charles River Laboratories Japan (Tokyo, Japan). The animals were housed in a temperature-, humidity-, and light- controlled room (12-h light and 12-h dark cycle) and allowed free access to water and chow. Five-week-old mice were fed either the standard chow (Oriental MF, 362 kcal/100 g, 5.4% energy as fat; Oriental Yeast, Tokyo, Japan) or high fat diet (D12492, 524 kcal/100 g, 60% energy as fat; Research Diets, New Brunswick, NJ) for 15 weeks. They were fasted for 1 h (12:00–13:00) and sacrificed to harvest the epididymal adipose tissue before (n = 10) and 2 weeks (n = 10), 4 weeks (n = 12), 6 weeks (n = 11), 8 weeks (n = 6), and 15 weeks (n = 4) after the experiments. All animal experiments were conducted according to the guidelines of Tokyo Medical and Dental University Committee on Animal Research (No. 0060026).

Histological Analysis—The epididymal WAT was fixed with neutral-buffered formalin and embedded in paraffin. Sections were stained with hematoxylin and eosin and studied under ×200 magnification to measure the adipocyte area using Win Roof software (Mitani Corporation, Tokyo, Japan) (19). Immunohistochemical study was carried out using 5-μm thick paraffin-embedded sections for macrophage marker F4/80 as previously described (20, 21).

Cell Culture—3T3-L1 preadipocytes (American Type Culture Collection, Manassas, VA) were maintained as described (6, 7). Differentiation of 3T3-L1 preadipocytes to adipocytes was described elsewhere (6, 7). Cells at day 8 and day 21 after the induction of differentiation were used as non-hypertrophied and hypertrophied adipocytes, respectively (6). Accumulation of triglyceride in adipocytes was detected by oil red O staining (19).

Measurement of Triglyceride Content—Triglyceride content in 3T3-L1 adipocytes was measured as previously reported (22). In brief, 3T3-L1 adipocytes in 35-mm dish were harvested, and cellular lipid was extracted by chloroform-methanol (2:1). After evaporation, precipitation was dissolved in isopropyl alcohol. Triglyceride content was measured using a colorimetric assay kit (triglyceride E-test Wako, Wako Pure Chemicals, Osaka, Japan) according to the manufacturer's instructions.

Quantitative Real-time PCR—Quantitative real-time PCR was performed with an ABI Prism 7000 Sequence Detection System using PCR Master Mix reagent kit (Applied Biosystems, Foster City, CA) as described (6, 19). Primers used were described in supplemental Table S1. Levels of mRNAs were normalized to those of housekeeping gene 36B4 mRNA.

ELISA—The MCP-1, IL-6, and adiponectin levels in culture supernatants were determined by the commercially available ELISA kits (MCP-1 and IL-6, R&D systems, Minneapolis, MN; adiponectin, Otsuka Pharmaceutical, Tokyo, Japan).

Immunoblot Assay—Nuclear and cytosolic extracts were prepared by using the Nuclear/Cytosol fractionation kit (BioVision, Mountain View, CA). Separation of nuclear and cytosolic proteins was confirmed by immunoblots with α-tubulin and lamin A/C antibodies, respectively. Whole cell lysates were prepared using buffer containing 50 mmol/liter HEPES (pH7.5), 150 mmol/liter NaCl, 100 mmol/liter sodium fluoride, 1 mmol/liter EGTA, 1 mmol/liter EDTA, 1% Triton X-100, 2 mmol/liter sodium vanadate, 2 mmol/liter phenylmethylsulfonyl fluoride, and protease inhibitor mixture (Sigma). Immunoblot assay was performed as described (6). Samples (10–20 μg protein/lane) were separated by 12.5% SDS-PAGE and electrophoretically transferred onto polyvinylidene difluoride filter membrane (PolyScreen; PerkinElmer, Wellesley, MA). After membranes were incubated with primary antibodies for 1 h at room temperature, immunoblots were developed with horseradish peroxidase-conjugated secondary antibodies (GE Healthcare Bio-Sciences, Piscataway, NJ) and a chemiluminescence kit (GE Healthcare Bio-Sciences). The signals were detected with LAS3000 (Fuji Photo Film, Tokyo, Japan).

Generation of 3T3-L1 Adipocytes Stably Expressing Coxsackie-Adenovirus Receptor (CAR)—A mouse CAR-expressing plasmid pcDNA3-CAR (23) was kindly provided by Dr. Hiroyuki Mizuguchi (National Institute of Biomedical Innovation, Osaka, Japan). The CAR retroviral expression vector (pMRX-CAR) was constructed by ligating the full-length CAR cDNA into the EcoR1 site of pMRX vector (24) and transfected into Plat-E packaging cells (25) using Lipofectamine2000 (Invitrogen) according to the manufacturer's instructions. Viral supernatants were harvested from 24 to 48 h after transfection and applied to 3T3-L1 adipocytes in Dulbecco's modified Eagle's medium containing 10% fetal bovine serum and 5 μg/ml of polybrene (Nacalai Tesque) in a final volume of 5 ml. The stable CAR-expressing 3T3-L1 adipocytes (CAR-3T3-L1 adipocytes) were obtained by 2 μg/ml of puromycin (Nacalai Tesque) selection.

Adenovirus-mediated Expression of MKP-1—The adenoviral vector expressing mouse MKP-1 (Ad-MKP-1) (26), kindly provided by Dr. Jeffery D. Molkentin (University of Cincinnati, Cincinnati, OH), was prepared using HEK293 cells and purified by VIRAPREP adenovirus purification kit (Virapur, LLC, San Diego, CA) as previously described (27). The GFP adenovirus (Ad-GFP; Clontech Laboratories, Palo Alto, CA) was used as a control. The CAR-3T3-L1 adipocytes at day 5 and day 18 after the induction of differentiation were transfected with Ad-MKP-1, incubated for 3 days, and harvested to be used for quantitative real-time PCR and immunoblot assay.

Statistical Analysis—Data are shown as means ± S.E. Statistical analysis was performed using the Student's *t* test and analysis of variance followed by Scheffe's test. $p < 0.05$ was considered statistically significant.

RESULTS

MCP-1 mRNA Expression in the Adipose Tissue from Mice with Diet-induced Obesity—Body weight was increased significantly in mice fed high fat diet for 2 weeks relative to those fed standard diet ($p < 0.01$) (Fig. 1*A*). The mice fed high fat diet weighed ~20% more than those fed standard diet for 15 weeks (29.7 ± 0.3 g *versus* 34.8 ± 1.9 g, $p < 0.05$). The weight of epididymal white adipose tissue (WAT) was significantly increased in mice fed high-fat diet for 2 weeks relative to those fed standard diet (0.26 ± 0.01 g *versus* 0.49 ± 0.04 g, $p < 0.01$). Histological examination revealed appreciable increase in adipocyte cell size in mice fed a high fat diet during the initial 2 weeks, which reached up to ~4-fold larger than that in mice fed standard diet after 15 weeks (Fig. 1*B*). There were no appreciable infiltration of macrophages in the adipose tissue up to 8 weeks after the experiment, after which interstitial cells stained with F4/80, a marker of activated macrophages, appeared in mice fed high fat diet (Fig. 1*C*). Correspondingly, F4/80 mRNA expression was also increased in the epididymal WAT in mice fed high fat diet for 15 weeks relative to those fed standard diet (Fig. 1*D*, *left*). In mice fed high fat diet, MCP-1 mRNA expression was increased as early as 4 weeks and gradually increased up to 15 weeks after the experiment (Fig. 1*D*, *right*). These observations indicate that MCP-1 mRNA expression is increased prior to macrophage infiltration at the early stage of obesity.

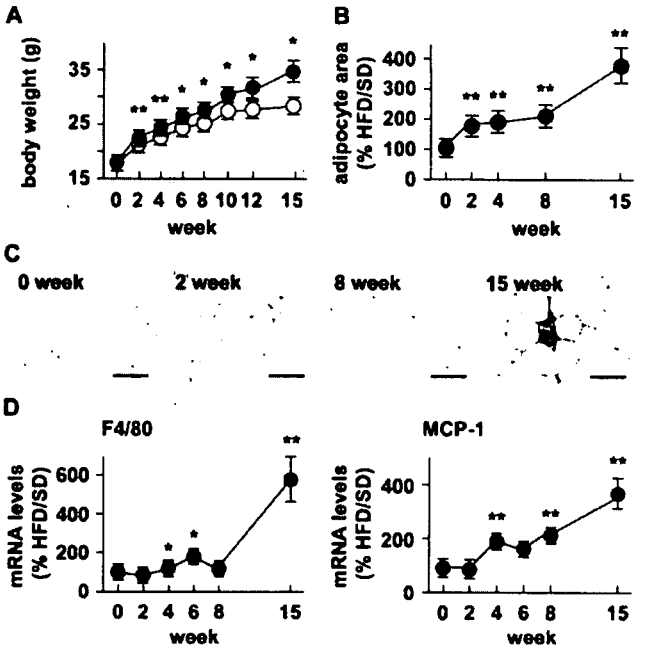

FIGURE 1. **Time course of adipocyte hypertrophy and macrophage infiltration in mice with diet-induced obesity.** Five-week-old male C57BL/6J mice were fed either SD or HFD for 15 weeks. *A*, time course of body weight. *Open circle*, SD; *closed circle*, HFD. *B*, time course of adipocyte area. *C*, macrophage marker F4/80 immunostaining of the epididymal WAT in diet-induced obese mice. Original magnification, ×200. *Scale bars*, 100 μm. *D*, time courses of F4/80 and MCP-1 mRNA expression. Data in *B* and *D* are expressed as the ratio of changes in mice fed HFD to those in mice fed SD. *, $p < 0.05$; **, $p < 0.01$ *versus* SD, $n = 4-12$ at each time point.

Dysregulation of Adipocytokine Production during the Course of Adipocyte Hypertrophy—To explore the molecular mechanisms underlying adipocyte hypertrophy, we cultured 3T3-L1 adipocytes up to 21 days after the induction of differentiation; they exhibited a gradual increase in lipid accumulation from day 8 to day 21 during the course of adipocyte hypertrophy as revealed by oil-red O staining (Fig. 2*A*) and triglyceride content (Fig. 2*B*). In this study, insulin-induced glucose uptake was preserved up to day 21 (supplemental Fig. S1).

Quantitative real-time PCR analysis revealed that MCP-1 mRNA expression was significantly increased up to day 21, ~6-fold higher than that in 3T3-L1 adipocytes (day 8) ($p < 0.01$), in parallel with increased cell size and lipid accumulation (Fig. 2*C*). Expression of IL-6 mRNA was also increased during the course of adipocyte hypertrophy. The IL-6 mRNA levels in 3T3-L1 adipocytes (day 21) were ~5-fold higher than those in 3T3-L1 adipocytes (day 8) ($p < 0.01$). By contrast, adiponectin mRNA expression showed significant reduction (up to 30%) during the course of adipocyte hypertrophy ($p < 0.01$). The MCP-1, IL-6, and adiponectin concentrations in the culture media were roughly parallel to their respective mRNA levels (Fig. 2*D*). The expression patterns of adipocytokines in hypertrophied 3T3-L1 adipocytes (day 21) were similar to those found in obese adipose tissue. We also confirmed that mRNA expression patterns of adipogenesis-related markers such as peroxisome proliferator-activated receptor γ2 (PPARγ2), adipocyte fatty acid-binding protein (aP2), fatty-acid transport protein 1 (FATP1), and CCAAT/enhancer-binding protein α

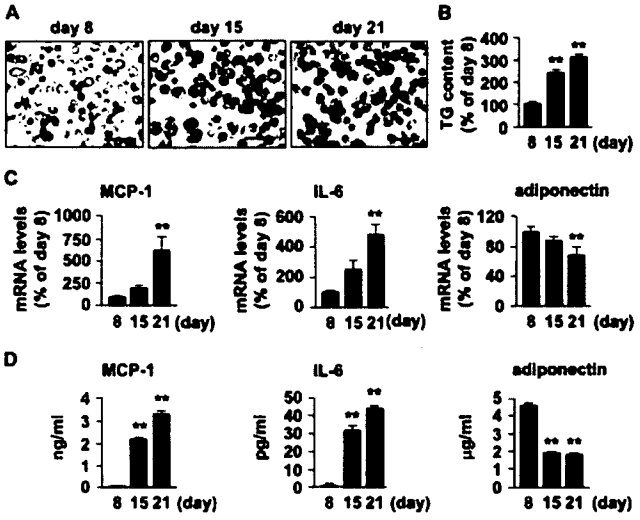

FIGURE 2. **Changes in adipocytokine expression during the course of adipocyte hypertrophy *in vitro*.** *A*, morphological changes of 3T3-L1 adipocytes during the course of adipocyte hypertrophy (day 8-day 21) as revealed by oil-red O staining. Original magnification, ×200. *Scale bars*, 100 μm. *B*, triglyceride accumulation in 3T3-L1 adipocytes during the course of adipocyte hypertrophy. *C* and *D*, changes in adipocytokine mRNA expression (*C*) and secretion (*D*) in 3T3-L1 adipocytes during the course of adipocyte hypertrophy. **, $p < 0.01$ *versus* day 8. $n = 4$.

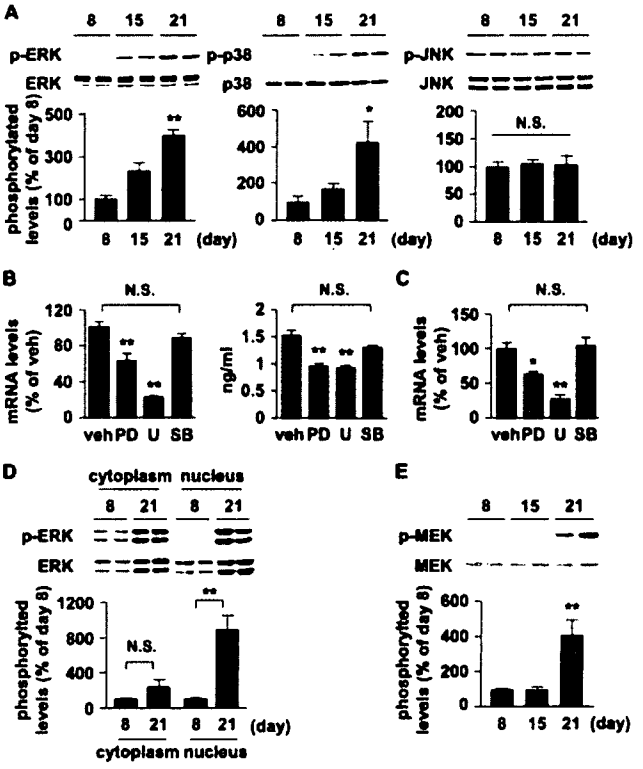

FIGURE 3. **Role of MAP kinases in MCP-1 mRNA expression in hypertrophied adipocytes.** *A*, phosphorylation of MAP kinases during the course of adipocyte hypertrophy. Representative immunoblots of ERK, p38 MAPK and JNK quantification of phosphorylation levels. *, $p < 0.05$; **, $p < 0.01$ *versus* day 8. $n = 4$. *B*, effect of 24-h-treatment with MAP kinase inhibitors on MCP-1 mRNA expression (*left*) and secretion (*right*) in hypertrophied 3T3-L1 adipocytes (day 21). *PD*, PD98059, 20 μmol/liter; *U*, U0126, 10 μmol/liter; *SB*, SB203580, 10 μmol/liter. **, $p < 0.01$ *versus* vehicle treated day 21. $n = 6$. *N.S.*, not significant. *C*, effect of 6-h-treatment with MAPK inhibitors on MCP-1 mRNA expression in hypertrophied 3T3-L1 adipocytes (day 21). *D*, phosphorylation of ERK in the cytosolic and nuclear fractions from non-hypertrophied (day 8) and hypertrophied (day 21) 3T3-L1 adipocytes. Representative immunoblots of ERK and quantification of phosphorylation levels. *E*, phosphorylation of MEK during the course of adipocyte hypertrophy. Representative immunoblots of MEK and quantification of phosphorylation levels. **, $p < 0.01$ *versus* day 8. $n = 4-6$.

(C/EBPα) in hypertrophied 3T3-L1 adipocytes were consistent with those in obese adipose tissue (supplemental Fig. S2). In this study, we used 3T3-L1 adipocytes cultured for 8 and 21 days after differentiation as non-hypertrophied (day 8) and hypertrophied (day 21) adipocytes, respectively.

Activation of MAPK Pathways during the Course of Adipocyte Hypertrophy—To explore the role of MAPK activation in the dysregulation of MCP-1 production during the course of adipocyte hypertrophy, we examined phosphorylation of ERK, p38 MAPK, and JNK in 3T3-L1 adipocytes during the course of adipocyte hypertrophy. Immunoblot analysis revealed that phosphorylation of ERK and p38 MAPK is increased in hypertrophied adipocytes relative to non-hypertrophied adipocytes (Fig. 3*A*). In this study, there was no significant induction of phosphorylation of JNK during the course of adipocyte hypertrophy (Fig. 3*A*). Treatment of hypertrophied adipocytes with MEK inhibitors, PD98059 and U0126, for 24 h significantly reduced MCP-1 mRNA levels (Fig. 3*B* left, $p < 0.01$) and secretion in the culture media (Fig. 3*B* right, $p < 0.01$). Moreover, the effect of the MEK inhibitors on MCP-1 mRNA expression was observed as early as 6 h after the treatment (Fig. 3*C*). Furthermore, phosphorylation of ERK was increased in the nuclear fraction rather than in the cytosolic fraction from hypertrophied adipocytes (Fig. 3*D*, $p < 0.01$). We also confirmed that phosphorylation of MEK is increased in hypertrophied adipocytes (Fig. 3*E*, $p < 0.01$). On the other hand, no such inhibitory effect was observed when treated with a p38 MAPK inhibitor, SB203580 (Fig. 3, *B* and *C*). These observations suggest that increased mRNA expression and secretion of MCP-1 in hypertrophied adipocytes are due at least in part to MEK-ERK activation.

MKP-1 Down-regulation during the Course of Adipocyte Hypertrophy—We next examined expression of members of the MKP family during the course of adipocyte hypertrophy. Interestingly, we detected substantial amounts of MKP-1 mRNA and protein in non-hypertrophied adipocytes, which are markedly down-regulated in hypertrophied adipocytes (Fig. 4, *A* and *B*, $p < 0.05$). There were no obvious changes in MKP-2 and MKP-3 mRNA levels during the course of adipocyte hypertrophy (Fig. 4*A*). We also observed that MKP-1 mRNA expression is significantly down-regulated in the adipose tissue from mice fed high fat diet for 2- and 4-weeks relative to those fed standard diet (Fig. 4*C*, $p < 0.05$). In addition, phosphorylation of ERK was significantly increased in the adipose tissue from mice that received 4-, 6-, 8-, and 15-week high fat diet relative to those fed standard diet (Fig. 4*D*, $p < 0.05$). These observations, taken together, suggest that MKP-1 is down-regulated in hypertrophied adipocytes, which is accompanied by ERK activation *in vivo*.

Generation of CAR-3T3-L1 Adipocytes—Because MKP-1 down-regulation may be responsible for the induction of MCP-1 during the course of adipocyte hypertrophy, we next examined the effect of MKP-1 restoration on ERK activity and

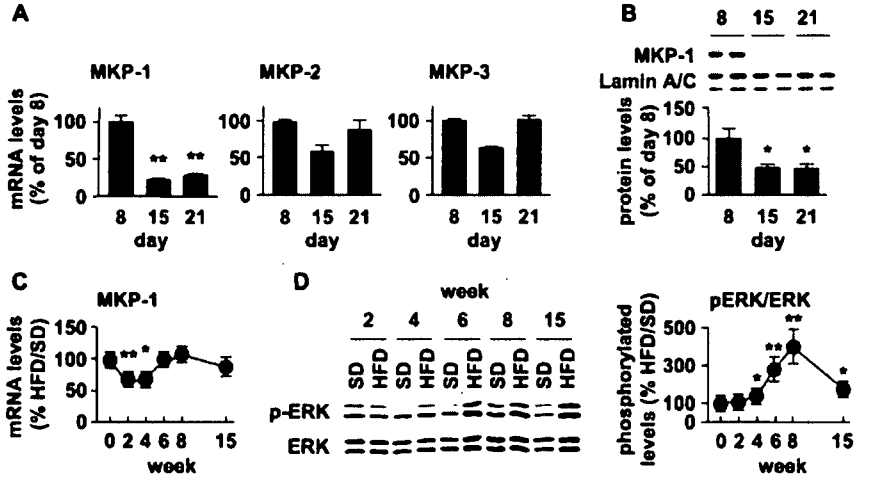

FIGURE 4. **Changes in MKP-1 expression during the course of adipocyte hypertrophy *in vitro* and *in vivo*.** *A*, changes in mRNA expression of MKP family during the course of adipocyte hypertrophy. $n = 6$. *B*, changes in MKP-1 protein levels in 3T3-L1 adipocytes during the course of adipocyte hypertrophy. Representative immunoblots of MKP-1 and quantification of protein levels. $n = 4$. *, $p < 0.05$; **, $p < 0.01$ *versus* day 8. *C* and *D*, time course of MKP-1 mRNA expression (*C*) and ERK phosphorylation (*D*) levels in mice with diet-induced obesity. Representative immunoblots of ERK and quantification of phosphorylation levels. Data in *C* and *D* are expressed as the ratio of changes in mice fed HFD to those in mice fed SD. *, $p < 0.05$; **, $p < 0.01$ *versus* SD. $n = 4$–12 at each time point.

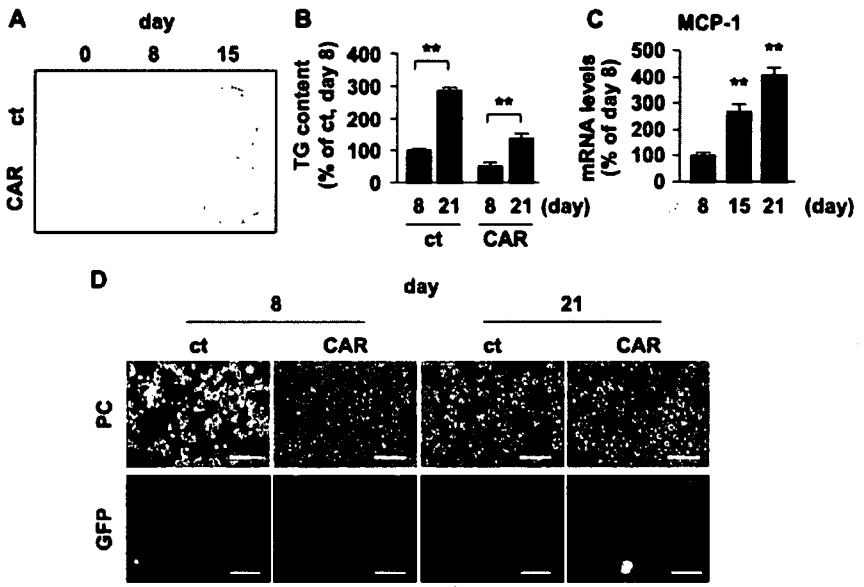

FIGURE 5. **Generation of 3T3-L1 adipocytes stably expressing CAR (CAR-3T3-L1 adipocytes).** *A* and *B*, lipid accumulation of CAR-3T3-L1 adipocytes and control 3T3-L1 adipocytes (*ct*) during the course of adipocyte differentiation and hypertrophy as revealed by oil-red O staining (*A*) and triglyceride content (*B*). *C*, changes in MCP-1 mRNA expression in CAR-3T3-L1 adipocytes. *D*, efficiency of adenovirus-mediated gene transfer in CAR-3T3-L1 adipocytes using Ad-GFP. *PC*, phase contrast view; *GFP*, GFP fluorescence view. Original magnification, ×200. *Scale bars*, 100 μm. **, $p < 0.01$ *versus* day 8. $n = 4$.

MCP-1 mRNA expression in hypertrophied adipocytes. Because hypertrophied 3T3-L1 adipocytes are difficult to transfect with plasmid- or even virally encoded genes, we generated CAR-3T3-L1 adipocytes as described under "Experimental Procedures." There was no obvious difference in lipid accumulation between CAR-3T3-L1 and 3T3-L1 adipocytes without retroviral infection (control 3T3-L1 adipocytes) (Fig. 5, *A* and *B*) during the course of adipocyte differentiation and hypertrophy. We also confirmed no appreciable difference in mRNA expression of adipogenesis-related markers and adipocytokines between the cells (supplemental Fig. S3). Similar to control 3T3-L1 adipocytes, CAR-3T3-L1 adipocytes exhibited the up-regulation of MCP-1 during the course of adipocyte hypertrophy (Fig. 5*C*). The transfection efficiency was markedly increased in CAR-3T3-L1 adipocytes relative to control 3T3-L1 adipocytes as judged by Ad-GFP infection (Fig. 5*D*).

Effect of MKP-1 Restoration in Hypertrophied Adipocytes—Infection with Ad-MKP-1 significantly increased MKP-1 mRNA expression in hypertrophied CAR-3T3-L1 adipocytes (Fig. 6*A*, *left*). We confirmed that MKP-1 protein levels in hypertrophied CAR-3T3-L1 adipocytes infected with Ad-MKP-1 are roughly comparable to those found in non-hypertrophied CAR-3T3-L1 adipocytes (Fig. 6*A*, *right*). In this setting, MKP-1 restoration in hypertrophied CAR-3T3-L1 adipocytes resulted in a marked reduction of ERK phosphorylation (Fig. 6*B*, $p < 0.05$) and MCP-1 mRNA expression (Fig. 6*C*, $p < 0.01$), which is roughly comparable to those found in non-hypertrophied CAR-3T3-L1 adipocytes. Interestingly, adiponectin mRNA expression was significantly increased and IL-6 mRNA expression tended to be reduced in hypertrophied CAR-3T3-L1 adipocytes with Ad-MKP-1 infection (supplemental Fig. S4), suggesting the anti-inflammatory effect of MKP-1 in hypertrophied adipocytes. Of note, there was no obvious difference in mRNA expression of adipogenesis-related markers by Ad-MKP-1 infection (supplemental Fig. S4). We also confirmed that Ad-MKP-1 infection does not affect lipid accumulation and insulin-induced glucose uptake in hypertrophied CAR-3T3-L1 (supplemental Fig. S5). These observations, taken together, indicate that restoration of MKP-1 does not affect adipocyte differentiation and hypertrophy but improves the overall inflammatory changes in hypertrophied adipocytes.

DISCUSSION

Recent studies showed that obese adipose tissue is characterized by increased infiltration of macrophages, suggesting that

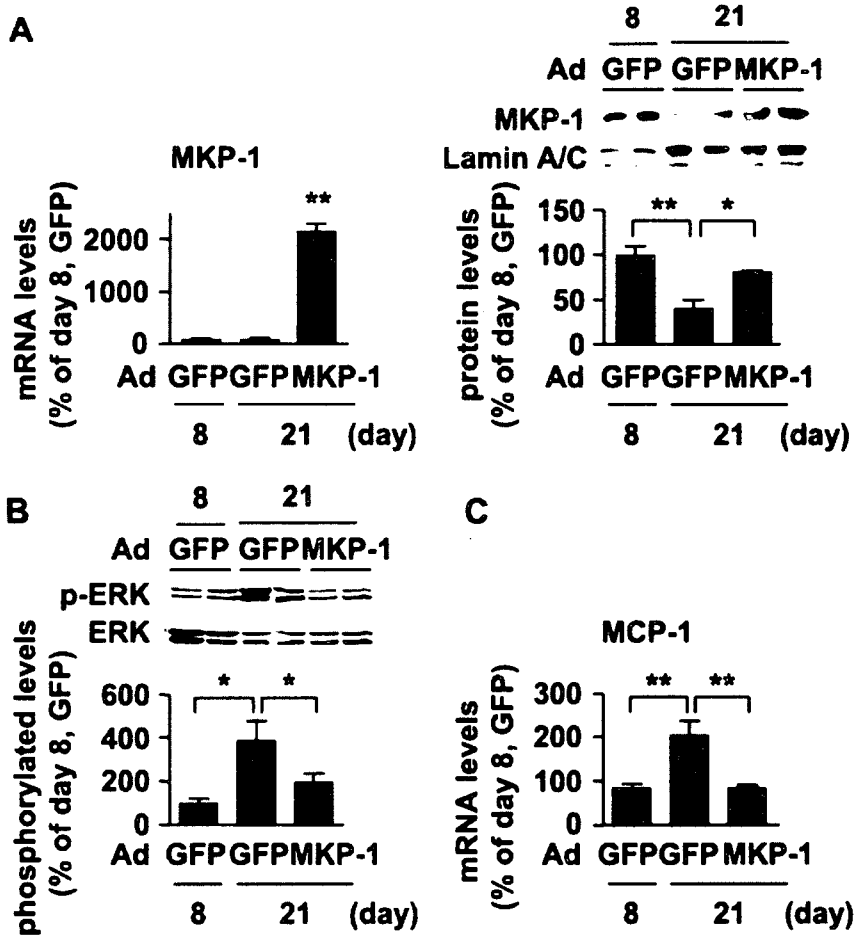

FIGURE 6. **Effect of MKP-1 restoration on ERK phosphorylation and MCP-1 mRNA expression in hypertrophied adipocytes.** *A*, adenovirus-mediated restoration of MKP-1 in hypertrophied CAR-3T3-L1 adipocytes (day 21). Changes in MKP-1 mRNA (*left*) and protein (*right*) expression. Representative immunoblots of MKP-1 and quantification of protein levels. *B* and *C*, effect of MKP-1 restoration on ERK phosphorylation (*B*) and MCP-1 mRNA expression (*C*). *, $p < 0.05$; **, $p < 0.01$ *versus* Ad-GFP, (day 21). $n = 6$.

the inflammatory changes induced by the cross-talk between adipocytes and macrophages are critical for the pathophysiology of obesity and thus the metabolic syndrome (4, 5). The molecular mechanisms underlying the recruitment of macrophages into obese adipose tissue have not fully been elucidated, but there is considerable evidence suggesting the involvement of MCP-1, which is increased during the course of obesity (8, 9). It is, therefore, important to know how MCP-1 is increased in hypertrophied adipocytes at the early stage of obesity, when macrophages are not infiltrated. This study was designed to elucidate the signaling pathway that mediates increased production of MCP-1 at the early stage of obesity.

In this study, we found that expression of MCP-1 mRNA is increased in the adipose tissue from mice rendered mildly obese by a short term high fat diet. Histologically, there is marked increase in adipocyte cell size with no obvious macrophage infiltration, suggesting that MCP-1 mRNA expression is increased in the adipose tissue prior to macrophage accumulation *in vivo*. Two recent studies with transgenic mice overexpressing MCP-1 in the adipose tissue and/or MCP-1-deficient mice showed that MCP-1 plays a role in the recruitment of macrophages into obese adipose tissue (11, 12). Furthermore, Weisberg *et al.* (28) reported the attenuation of macrophage content and inflammatory changes in the adipose tissue from mice lacking C-C motif chemokine receptor-2, a major receptor for MCP-1, during a long term high fat diet. Together with recent evidence that MCP-1 mRNA expression and secretion in primary cultured adipocytes from obese subjects are positively correlated with their cell size (29), our data herein support the concept that increased production of MCP-1 in hypertrophied adipocytes at the early stage of obesity contributes to increased infiltration of macrophages into the adipose tissue at the late stage of obesity.

There are multiple intracellular signaling pathways activated in adipocytes during the course of adipocyte hypertrophy. The data of this study demonstrate that 3T3-L1 adipocytes, when cultured alone up to 21 days after differentiation, is capable of up-regulating MCP-1 and IL-6 and down-regulating adiponectin in parallel with increased cell size and lipid accumulation, which are comparable to those in obese adipose tissue. Moreover, mRNA expression patterns of some adipogenesis-related markers are also roughly parallel to those in obese adipose tissue, suggesting that 3T3-L1 adipocytes cultured from day 8 to day 21 serve as the useful *in vitro* experimental model system to investigate the molecular mechanism for the dysregulation of adipocytokine production during the course of adipocyte hypertrophy.

In this study, we observed that ERK and p38 MAPK are activated in hypertrophied 3T3-L1 adipocytes. Moreover, increased production of MCP-1 is significantly suppressed by MEK inhibitors as early as 6 h after the treatment, but not by a p38 MAPK inhibitor. We also demonstrated that ERK phosphorylation is significantly increased in the nuclear fraction but not in cytosolic fraction obtained from non-hypertrophied (day 8) and hypertrophied (day 21) 3T3-L1 adipocytes, suggesting that ERK activation occurs mostly in the nucleus rather than in the cytoplasm of adipocytes during the course of adipocyte hypertrophy. These observations are consistent with the concept that MKP-1 acts as a negative regulator of MAPKs within the nucleus (30). Furthermore, we observed that phosphorylation of MEK is increased in hypertrophied adipocytes. Together with a recent report that MAPKs are involved in the regulation of MCP-1 in human adipose tissue (31), these observations suggest that increased production of MCP-1 in hypertrophied adipocytes is mediated at least in part thorough MEK-ERK activa-

tion. In this regard, using the TRANSFAC (6.0) data base, we also searched for transcriptional factor binding sites in the mouse, rat, and human MCP-1 promoter and found a consensus AP-1 binding site 3–4-kb upstream of the transcriptional start site. Moreover, there are previous reports showing that cytokine-induced MCP-1 is mediated at least in part through the activation of ERK and AP-1 (32, 33). It is, therefore, conceivable that decrease in MKP-1 leads to the activation of ERK and AP-1 transcriptional activity within the nucleus, thereby increasing MCP-1 production during the course of adipocyte hypertrophy.

In this study, we demonstrate for the first time that both MKP-1 mRNA and protein levels are significantly down-regulated during the course of adipocyte hypertrophy *in vitro*. Moreover, restoration of MKP-1 in hypertrophied adipocytes reduces the otherwise increased ERK phosphorylation and thus MCP-1 mRNA expression. These observations, taken together, suggest that ERK activation through MKP-1 down-regulation is involved in increased production of MCP-1 in 3T3-L1 adipocytes during the course of adipocyte hypertrophy. The above discussion is consistent with the *in vivo* observation that ERK is activated, which is followed by MKP-1 down-regulation in the adipose tissue at the early stage of obesity, when there is no appreciable macrophage infiltration. Thus, reduced MKP-1 expression may be one of the early events during the progression of obesity *in vivo*, thereby leading to increased production of MCP-1 through the activation of ERK. In this regard, constitutive activation of ERK as a result of low induction of MKP-1 confers stronger resistance of immortalized cells than that of normal human fibroblasts to a cancer therapy called photodynamic therapy (34, 35). It is also noteworthy that MKP-1 expression is down-regulated in human ovarian cancer cell lines, where its forced re-expression reduces their malignant potential, suggesting the role of MKP-1 in the progression of human ovarian cancer (36). Thus, imbalance between MKP-1 and MEK activities as a result of MKP-1 down-regulation may cause ERK activation, thereby leading to increased production of MCP-1 in hypertrophied adipocytes.

It is also important to know the upstream signaling pathways responsible for MKP-1 down-regulation during the course of adipocyte hypertrophy. Recent studies have suggested the involvement of multiple intracellular signaling pathways in the inflammatory changes in adipocytes *in vitro* and in obese adipose tissue *in vivo*. For instance, Özcan *et al.* (37) reported that obesity is associated with the induction of ER stress predominantly in the adipose tissue and liver and demonstrated that ER stress is a central feature of obesity-related insulin resistance and type 2 diabetes. On the other hand, Furukawa *et al.* showed that ROS production is increased in parallel with lipid accumulation in 3T3-L1 adipocytes and that oxidative stress induces the dysregulation of adipocytokine production (38). It is, therefore, interesting to investigate the relationship among ER stress induction, ROS production, and MKP-1 activation during the course of adipocyte hypertrophy and/or at the early stage of obesity. Lin *et al.* (39, 40) demonstrated previously that MKP-1 degradation via the ubiquitin-proteasome pathway is stimulated by ERK, thereby leading to the sustained activation of ERK. Whether MKP-1 is thus down-regulated in hypertrophied adipocytes or not must await further investigations.

During the course of this study, Wu *et al.* (41) have reported that mice deficient in MKP-1 (MKP-1$^{-/-}$ mice) exhibit enhanced MAPK activity in the adipose tissue, reduced adipocyte cell size relative to wild-type littermates, and resistance to diet-induced obesity as a result of increased lipid metabolism in the liver and oxygen consumption in the skeletal muscle. Using mice with congenital deficiency of MKP-1, however, the authors did not address the role of MKP-1 in adipocytes during the course of adipocyte hypertrophy or at the early stage of obesity. In this regard, Bost *et al.* (17) reported that ERK1$^{-/-}$ mice have decreased adiposity and fewer adipocytes than wild-type littermates, and are resistant to high fat diet-induced obesity and insulin resistance. In this study, we demonstrated that ERK activation through the down-regulation of MKP-1 plays a role in increased production of MCP-1 in hypertrophied adipocytes during the course of obesity. It is, therefore, tempting to speculate that ERK activation through the down-regulation of MKP-1 plays an important role in the regulation of adipocyte differentiation, adiposity, and high fat diet-induced obesity *in vivo*. In this study, we also found that restoration of MKP-1 improves the dysregulation of adipocytokine production in hypertrophied adipocytes, which may improve obesity-related insulin resistance via adipocytokine mechanism *in vivo*. The pathophysiologic role of MKP-1 down-regulation in hypertrophied adipocytes at the early stage of obesity *in vivo* must await further investigation.

To obtain hypertrophied 3T3-L1 adipocytes whose MKP-1 levels are restored to those of non-hypertrophied 3T3-L1, we tried to produce 3T3-L1 adipocytes stably expressing MKP-1 using the retrovirus vector and observed that they are unable to differentiate into lipid-laden mature adipocytes.[4] This is consistent with the concept that ERK should be on and off properly during adipogenesis *in vitro* (16, 42). Although the adenoviral vector has been widely used for the introduction of exogenous genes in non-proliferating cells, 3T3-L1 adipocytes, particularly when hypertrophied, are transfected with less efficiency because of the scarcity of CAR (43–45). In this study, we generated 3T3-L1 adipocytes stably expressing CAR (or CAR-3T3-L1 adipocytes), which is infected with the adenoviral expression vector with ease, even after being hypertrophied. Importantly, there are no appreciable differences in adipogenesis, lipid accumulation, and adipocytokine expression during the course of adipocyte differentiation and hypertrophy between CAR-3T3-L1 adipocytes and control 3T3-L1 adipocytes. This study has verified the usefulness of CAR-3T3-L1 adipocytes as the unique experimental tool to investigate the molecular basis for adipocyte differentiation and hypertrophy.

In conclusion, this study represents the first demonstration that ERK activation through MKP-1 down-regulation is involved in increased production of MCP-1 in adipocytes at the early stage of obesity. The data of this study suggest that MKP-1 activation may offer a novel therapeutic strategy to reduce the otherwise increased production of MCP-1 in hypertrophied

[4] A. Ito, T. Suganami, and Y. Ogawa, unpublished data.

adipocytes at the early stage of obesity and thus macrophage infiltration into the adipose tissue at the late stage of obesity.

Acknowledgments—We thank Dr. Hiroshi Nishina for critical reading of the manuscript. We thank Dr. Toshio Kitamura for Plat-E, Dr. Hiroyuki Mizuguchi for pcDNA3-CAR, Dr. Shoji Yamaoka for pMRX, and Dr. Jeffery D. Molkentin for MKP-1 adenoviral expression vector. We are also grateful to the members of the Ogawa laboratory for discussions.

REFERENCES

1. Dandona, P., Aljada, A., and Bandyopadhyay, A. (2004) *Trends Immunol.* **25,** 4–7
2. Wellen, K. E., and Hotamisligil, G. S. (2005) *J. Clin. Investig.* **115,** 1111–1119
3. Berg, A. H., and Scherer, P. E. (2005) *Circ. Res.* **96,** 939–949
4. Weisberg, S. P., McCann, D., Desai, M., Rosenbaum, M., Leibel, R. L., and Ferrante, A. W., Jr. (2003) *J. Clin. Investig.* **112,** 1796–1808
5. Xu, H., Barnes, G. T., Yang, Q., Tan, G., Yang, D., Chou, C. J., Sole, J., Nichols, A., Ross, J. S., Tartaglia, L. A., and Chen, H. (2003) *J. Clin. Investig.* **112,** 1821–1830
6. Suganami, T., Nishida, J., and Ogawa, Y. (2005) *Arterioscler. Thromb. Vasc. Biol.* **25,** 2062–2068
7. Suganami, T., Tanimoto-Koyama, K., Nishida, J., Itoh, M., Yuan, X., Mizuarai, S., Kotani, H., Yamaoka, S., Miyake, K., Aoe, S., Kamei, Y., and Ogawa, Y. (2007) *Arterioscler. Thromb. Vasc. Biol.* **27,** 84–91
8. Chen, A., Mumick, S., Zhang, C., Lamb, J., Dai, H., Weingarth, D., Mudgett, J., Chen, H., MacNeil, D. J., Reitman, M. L., and Qian, S. (2005) *Obes. Res.* **13,** 1311–1320
9. Takahashi, K., Mizuarai, S., Araki, H., Mashiko, S., Ishihara, A., Kanatani, A., Itadani, H., and Kotani, H. (2003) *J. Biol. Chem.* **278,** 46654–46660
10. Cancello, R., Henegar, C., Viguerie, N., Taleb, S., Poitou, C., Rouault, C., Coupaye, M., Pelloux, V., Hugol, D., Bouillot, J. L., Bouloumie, A., Barbatelli, G., Cinti, S., Svensson, P. A., Barsh, G. S., Zucker, J. D., Basdevant, A., Langin, D., and Clement, K. (2005) *Diabetes* **54,** 2277–2286
11. Kamei, N., Tobe, K., Suzuki, R., Ohsugi, M., Watanabe, T., Kubota, N., Ohtsuka-Kowatari, N., Kumagai, K., Sakamoto, K., Kobayashi, M., Yamauchi, T., Ueki, K., Oishi, Y., Nishimura, S., Manabe, I., Hashimoto, H., Ohnishi, Y., Ogata, H., Tokuyama, K., Tsunoda, M., Ide, T., Murakami, K., Nagai, R., and Kadowaki, T. (2006) *J. Biol. Chem.* **281,** 26602–26614
12. Kanda, H., Tateya, S., Tamori, Y., Kotani, K., Hiasa, K., Kitazawa, R., Kitazawa, S., Miyachi, H., Maeda, S., Egashira, K., and Kasuga, M. (2006) *J. Clin. Investig.* **116,** 1494–1505
13. Johnson, G. L., and Lapadat, R. (2002) *Science* **298,** 1911–1912
14. Farooq, A., and Zhou, M. M. (2004) *Cell. Signal.* **16,** 769–779
15. Keyse, S. M. (2000) *Curr. Opin. Cell Biol.* **12,** 186–192
16. Sakaue, H., Ogawa, W., Nakamura, T., Mori, T., Nakamura, K., and Kasuga, M. (2004) *J. Biol. Chem.* **279,** 39951–39957
17. Bost, F., Aouadi, M., Caron, L., Even, P., Belmonte, N., Prot, M., Dani, C., Hofman, P., Pages, G., Pouyssegur, J., Le Marchand-Brustel, Y., and Binetruy, B. (2005) *Diabetes* **54,** 402–411
18. Rosen, E. D., and MacDougald, O. A. (2006) *Nat. Rev. Mol. Cell Biol.* **7,** 885–896
19. Kouyama, R., Suganami, T., Nishida, J., Tanaka, M., Toyoda, T., Kiso, M., Chiwata, T., Miyamoto, Y., Yoshimasa, Y., Fukamizu, A., Horiuchi, M., Hirata, Y., and Ogawa, Y. (2005) *Endocrinology* **146,** 3481–3489
20. Suganami, T., Mieda, T., Itoh, M., Shimoda, Y., Kamei, Y., and Ogawa, Y. (2007) *Biochem. Biophys. Res. Commun.* **354,** 45–49
21. Iinnouchi, K., Terasaki, Y., Fujiyama, S., Tomita, K., Kuziel, W. A., Maeda, N., Takahashi, K., and Takeya, M. (2003) *J. Pathol.* **200,** 406–416
22. Kamon, J., Naitoh, T., Kitahara, M., and Tsuruzoe, N. (2001) *Cell. Signal* **13,** 105–109
23. Hosono, T., Mizuguchi, H., Katayama, K., Koizumi, N., Kawabata, K., Yamaguchi, T., Nakagawa, S., Watanabe, Y., Mayumi, T., and Hayakawa, T. (2005) *Gene (Amst.)* **348,** 157–165
24. Saitoh, T., Nakayama, M., Nakano, H., Yagita, H., Yamamoto, N., and Yamaoka, S. (2003) *J. Biol. Chem.* **278,** 36005–36012
25. Morita, S., Kojima, T., and Kitamura, T. (2000) *Gene Ther.* **7,** 1063–1066
26. Bueno, O. F., De Windt, L. J., Lim, H. W., Tymitz, K. M., Witt, S. A., Kimball, T. R., and Molkentin, J. D. (2001) *Circ. Res.* **88,** 88–96
27. Suganami, E., Takagi, H., Ohashi, H., Suzuma, K., Suzuma, I., Oh, H., Watanabe, D., Ojima, T., Suganami, T., Fujio, Y., Nakao, K., Ogawa, Y., and Yoshimura, N. (2004) *Diabetes* **53,** 2443–2448
28. Weisberg, S. P., Hunter, D., Huber, R., Lemieux, J., Slaymaker, S., Vaddi, K., Charo, I., Leibel, R. L., and Ferrante, A. W., Jr. (2006) *J. Clin. Investig.* **116,** 115–124
29. Skurk, T., Alberti-Huber, C., Herder, C., and Hauner, H. (2006) *J. Clin. Endocrinol. Metab.* **92,** 1023–1033
30. Camps, M., Nichols, A., and Arkinstall, S. (2000) *FASEB J.* **14,** 6–16
31. Fain, J. N., and Madan, A. K. (2005) *Int. J. Obes. (Lond.)* **29,** 1299–1307
32. Marumo, T., Schini-Kerth, V. B., and Busse, R. (1999) *Diabetes* **48,** 1131–1137
33. Yoshimura, H., Nakahama, K., Safronova, O., Tanaka, N., Muneta, T., and Morita, I. (2006) *Inflamm. Res.* **55,** 543–549
34. Barry, O. P., Mullan, B., Sheehan, D., Kazanietz, M. G., Shanahan, F., Collins, J. K., and O'Sullivan, G. C. (2001) *J. Biol. Chem.* **276,** 15537–15546
35. Tong, Z., Singh, G., and Rainbow, A. J. (2002) *Cancer Res.* **62,** 5528–5535
36. Manzano, R. G., Montuenga, L. M., Dayton, M., Dent, P., Kinoshita, I., Vicent, S., Gardner, G. J., Nguyen, P., Choi, Y. H., Trepel, J., Auersperg, N., and Birrer, M. J. (2002) *Oncogene* **21,** 4435–4447
37. Özcan, U., Cao, Q., Yilmaz, E., Lee, A. H., Iwakoshi, N. N., Ozdelen, E., Tuncman, G., Gorgun, C., Glimcher, L. H., and Hotamisligil, G. S. (2004) *Science* **306,** 457–461
38. Furukawa, S., Fujita, T., Shimabukuro, M., Iwaki, M., Yamada, Y., Nakajima, Y., Nakayama, O., Makishima, M., Matsuda, M., and Shimomura, I. (2004) *J. Clin. Investig.* **114,** 1752–1761
39. Lin, Y. W., Chuang, S. M., and Yang, J. L. (2003) *J. Biol. Chem.* **278,** 21534–21541
40. Lin, Y. W., and Yang, J. L. (2006) *J. Biol. Chem.* **281,** 915–926
41. Wu, J. J., Roth, R. J., Anderson, E. J., Hong, E. G., Lee, M. K., Choi, C. S., Neufer, P. D., Shulman, G. I., Kim, J. K., and Bennett, A. M. (2006) *Cell Metab.* **4,** 61–73
42. Prusty, D., Park, B. H., Davis, K. E., and Farmer, S. R. (2002) *J. Biol. Chem.* **277,** 46226–46232
43. Orlicky, D. J., DeGregori, J., and Schaack, J. (2001) *J. Lipid Res.* **42,** 910–915
44. Orlicky, D. J., and Schaack, J. (2001) *J. Lipid Res.* **42,** 460–466
45. Ross, S. A., Song, X., Burney, M. W., Kasai, Y., and Orlicky, D. J. (2003) *Biochem. Biophys. Res. Commun.* **302,** 354–358

The endothelial nitric oxide synthase gene -786T/C polymorphism is a predictive factor for reattacks of coronary spasm

Tsunenori Nishijima[a], Masafumi Nakayama[a], Michihiro Yoshimura[a], Koji Abe[a], Megumi Yamamuro[a], Satoru Suzuki[a], Makoto Shono[a], Seigo Sugiyama[a], Yoshihiko Saito[c], Yoshihiro Miyamoto[d], Kazuwa Nakao[e], Hirofumi Yasue[b] and Hisao Ogawa[a]

Objective **We previously found a -786T/C polymorphism in the 5′-flanking region of the endothelial nitric oxide synthase (eNOS) gene and reported that this polymorphism is strongly associated with coronary spasm. In this study, we examined whether the polymorphism is a prognostic marker in coronary spasm patients.**

Methods and results **We examined the clinical courses of 201 consecutive patients with coronary spasm who were admitted to our institution: 146 patients with the -786T/T genotype; 50 patients with the -786C/T genotype; and five patients with the -786C/C genotype. The mean follow-up period was 76±60 months. All the patients took calcium channel blockers and/or nitrate during the follow-up period. In this study, no patients died due to a cardiac event. About 25 patients were readmitted owing to cardiovascular disease. Out of these 25 patients, 23 patients were readmitted owing to a reattack of coronary spasm. The -786C allele was significantly associated with readmission due to coronary spasm ($P=0.0072$, odds ratio: 3.37 in the dominant effect). Kaplan–Meier analysis revealed that the occurrence of readmission was significantly higher in the patients with the -786C allele than in the patients without the -786C allele ($P=0.0079$). Further, multiple logistic regression analysis revealed that the -786T/C polymorphism was an independent predictor for readmission due to reattack of coronary spasm ($P=0.006$; relative risk=3.590).**

Conclusions **The eNOS -786C allele is an independent risk factor for readmission due to a recurrent attack of coronary spasm in patients with coronary spasm, even if the patients have taken calcium channel blockers and/or nitrate.** ***Pharmacogenetics and Genomics*** **17:581–587 © 2007 Lippincott Williams & Wilkins.**

Pharmacogenetics and Genomics 2007, 17:581–587

Keywords: coronary disease, coronary spasm, genes, nitric oxide synthase, prognosis

[a]The Department of Cardiovascular Medicine, Graduate School of Medical Sciences, Kumamoto University, [b]Division of Cardiology, Kumamoto Aging Research Institute, Kumamoto, [c]First Department of Internal Medicine, Nara Medical University, Kashihara, Nara, [d]Division of Atherosclerosis and Diabetes, National Cardiovascular Center, Suita, Osaka and [e]Department of Medicine and Clinical Science, Kyoto University Graduate School of Medicine, Sakyou-ku, Kyoto, Japan

Correspondence to Dr Michihiro Yoshimura, MD, Department of Cardiovascular Medicine, Graduate School of Medical Sciences, Kumamoto University, 1-1-1 Honjo, Kumamoto 860-8556, Japan
Tel: +81 96 373 5175; fax: +81 96 362 3256;
e-mail: bnp@kumamoto-u.ac.jp

Received 24 May 2006 Accepted 8 August 2006

Introduction

Coronary spasm plays an important role in the pathogenesis of not only variant angina but also ischemic heart diseases in general, including other forms of angina pectoris, acute myocardial infarction, and sudden death [1–3].

We previously reported that the long-term prognosis for patients with coronary spasm is relatively good and that the use of calcium channel blockers (CCBs) improves it [4,5].

We have recommended that patients with coronary spasm take CCB, which dilates the large coronary arteries and thereby prevents the occurrence of coronary spasm; however, there were many patients who were readmitted owing to a recurrent attack of coronary spasm while on the CCB regimen [6]. It is not yet clear what factor(s) predisposes coronary-spasm patients who take CCB to a reattack of coronary spasm.

We previously reported that a -786T/C polymorphism in the 5′-flanking region of the endothelial nitric oxide synthase (eNOS) gene is strongly associated with coronary spasm; it also results in a significant reduction in eNOS gene promoter activity [7]. We further showed that the replication protein A1 binds to the -786C allele and thereby represses eNOS gene transcription [8]. Our clinical research revealed that the polymorphism strongly increases the basal tone of the coronary arteries, and enhances their response to the constrictor effects of acetylcholine (ACh) [9,10]; furthermore, we reported

1744-6872

that the polymorphism is significantly associated with myocardial infarction, especially in patients without coronary stenosis [11]. These findings suggest that the -786T/C polymorphism in the eNOS gene compromises endothelial NO synthesis and thereby predisposes the patients to severe coronary spasm.

In this study, we examined the association between the -786T/C polymorphism and the long-term prognosis for coronary-spasm patients.

Methods

Study population

The study population consisted of 201 consecutively admitted patients from July 1984 to July 2000 (100 men; 101 women: mean age in years, 61.9; range 25–81 years) from whom genomic DNA could be obtained. All of them had coronary spasm as defined by an intracoronary injection of ACh. Coronary spasm was defined as total or subtotal occlusion of a coronary artery, which was associated with ischemic electrocardiographic changes and/or chest pain. Patients with significant organic stenosis in the coronary arteries, defined as having more than 50% organic stenosis in at least one coronary artery after nitroglycerine administration, were excluded. Patients who stopped medications were excluded from this study.

The patients were divided into two groups: the -786T group consisting of 146 patients with the -786T/T genotype (74 men and 72 women; mean age in years, 61.7; range, 25–81) and the -786C group consisting of 55 patients (28 men and 27 women; mean age in years, 62.2; range, 40–77). The latter group included 50 patients with the -786C/T genotype and five patients with the -786C/C genotype. We examined the following two events during the follow-up period: (i) death from all causes and (ii) readmission due to a coronary arterial event, such as reattack of coronary spastic angina, angina pectoris due to organic stenosis, or acute myocardial infarction.

Cardiac catheterization

All medications taken by the study participants were discontinued at least 48 h before cardiac catheterization. Coronary arteriography was performed in the morning while the patients were in a fasting state. After baseline arteriography of the left and right coronary arteries, an intracoronary injection of ACh was administered as described previously [12–15].

Two consecutive doses (50 and 100 μg) of ACh were administered 4 min apart, injected into the left coronary artery: angiography was performed within 30 s of each injection. Then, 50 μg of ACh was injected into the right coronary artery and angiography was again performed. Finally, both left and right coronary arteriograms were taken after an intracoronary injection of 1 mg of isosorbide dinitrate. We evaluated the degree of organic stenosis after the injection of isosorbide dinitrate.

Screening method for the -786T/C polymorphism in the endothelial nitric oxide synthase gene

An allele-specific oligonucleotide method was used in the screening for the -786T/C polymorphism in the eNOS gene. Hybridization was accomplished with ^{32}P-radiolabeled oligonucleotides corresponding to either the probe for the -786T allele or the probe for the -786C allele. The method has been described earlier. [7]. In brief, the PCR fragments, 236-bp in length, including the -786T/C polymorphism site, were blotted in duplicate onto nylon membranes. Hybridization was accomplished with ^{32}P-radiolabeled oligonucleotides corresponding to either the -786T sequence (5′-GGG TCA GCC AGC CAG GGAA-3′; probe for the -786T sequence) or the -786C sequence (5′-GGG TCA GCCGGC CAG GGAA-3′; probe for the -786C sequence).

Statistical analysis

Continuous variables are expressed as mean ± SD. Mean values were compared using the unpaired Student's *t*-test. The χ^2 test was used for the evaluation of differences between proportions. A probability value < 0.05 was considered to indicate statistical significance.

Multiple logistic regression analysis with forward stepwise selection was performed with SPSS 14.0J for Windows (SPSS Japan Inc). Multiple logistic analysis was used to determine independent predictors of coronary spasms. Independent variables were coded as the following dummy variables: genotype, 0 for the -786T/T genotype and 1 for the -786C/T or the -786C/C genotype; sex, 0 for women and 1 for men; age, 0 for < 55 years and 1 for ≥ 55 years; body mass index, 0 for $< 25\,kg/m^2$ and 1 for $\geq 25\,kg/m^2$; hypercholesterolemia, 0 for < 220 mg/dl and 1 for ≥ 220 mg/dl; Cigarette smoking, 0 for nonsmokers and 1 for ex-smokers (all study participants quit smoking upon admission); hypertension, 0 for normotension and 1 for hypertension; and diabetes mellitus, 0 for an absence and 1 for a presence. A Kaplan–Meier survival curve was used for determining survival and readmission rates in both the -786T group and the -786C group. We compared the survival rates and readmission rates between the -786T group and the -786C group using the log-rank test.

Results

Follow-up periods

The patients in this study were followed up until 1 December 2005. The mean follow-up period was 76 ± 60 months (range 1–252 months) for all study patients, with mean follow-up periods of 74 ± 56 months (range 1–252 months) for the -786T group and 81 ± 68 months (range 1–235 months) for the -786C group.

Clinical characteristics in the study patients

The clinical characteristics of the study patients are shown in Table 1. The incidence of coronary risk factors, including age, sex, hypertension, and cigarette smoking, were compared between the -786T and the -786C groups. No significant differences were seen in these coronary risk factors between the -786T and the -786C groups. No significant differences were seen in the drug regimens, including CCB, nitrates, angiotensin-converting enzyme inhibitors (ACE-I), or antiplatelets between the two groups.

Prognosis of patients and causes of death

In this study population, 192 survived and nine died during the follow-up period. Of the nine patients who died, three died of lung cancer, one of pancreas cancer, one of a brain tumor, one of a ruptured thoracic aortic aneurysm, one of stroke, and two of respiratory failure. Kaplan–Meier analysis revealed that there were no significant differences in the death rates between the -786T group and the -786C group (log-rank test: $P = 0.5945$) (Fig. 1).

Readmission due to coronary arterial disease and the -786T/C polymorphism

Twenty-five patients were readmitted owing to a recurrence of coronary arterial disease. Out of these 25 patients, 23 patients were readmitted owing to a reattack of coronary spasm. In the patients readmitted owing to a reattack of coronary spasm, one patient was readmitted owing to acute myocardial infarction without significant organic stenosis. He had the -786C/C genotype of the eNOS gene. Two patients who were readmitted owing to a progression of coronary stenosis had the -786T/T genotypes.

The rate of readmission due to coronary arterial disease was significantly higher in the -786C group than in the -786T group ($P = 0.0134$) [21.8% (12/55) and 8.9% (13/146), respectively, as is shown in Table 2]. The rate of readmission due to a reattack of coronary spasm was significantly higher in the -786C group than in the -786T group ($P = 0.0046$) [21.8% (12/55) and 7.5% (11/146), respectively].

Table 1 **Clinical characteristics of the study patients**

	-786T group ($n = 146$)	-786C group ($n = 55$)	*P* value
Age (years)	62 ± 11	62 ± 10	NS
Men/women	72/74	28/27	NS
Hypertension	44/146 (30%)	15/55 (27%)	NS
Cigarette smoking	78/146 (53%)	33/55 (60%)	NS
Diabetes mellitus	28/146 (19%)	11/55 (20%)	NS
Hypercholesterolemia	41/146 (28%)	13/55 (24%)	NS
BMI (kg/m^2)	23 ± 3	23 ± 3	NS
Pharmacotherapy			
CCB	137/146 (94%)	52/55 (95%)	NS
Nitrates	20/146 (14%)	4/55 (7%)	NS
ACE-I	12/146 (8%)	7/55 (13%)	NS
Antiplatelet	16/146 (11%)	6/55 (11%)	NS
HMG-CoA Reductase inhibitor	18/146 (12%)	2/55 (4%)	NS

Values are numbers of patients or mean ± SD.
ACE-I, angiotensin-converting enzyme inhibitor; BMI, body mass index; CCB, calcium channel blocker; NS, not significant.

Fig. 1

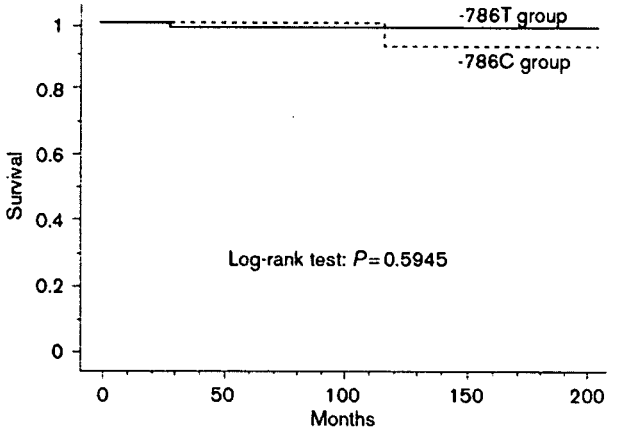

Kaplan–Meier survival curves of cumulative death rates in patients with coronary spasm divided into two groups according to the -786T/C polymorphism.

Table 2 **Readmission rates**

	-786T group ($n = 55$)	-786C group ($n = 146$)	*P* value
Reattack of coronary spasm	11/146 (7.5%)	12/55 (21.8%)	0.0046
Progression of coronary stenosis	2/146 (1.4%)	0/55 (0%)	0.3830
Total	13/146 (8.9%)	12/55 (21.8%)	0.0134

Values are numbers of patients.

Kaplan–Meier analysis revealed that the occurrence of readmission due to coronary arterial disease was significantly lower in the -786T group than in the -786C group ($P = 0.0079$) (Fig. 2). Further, the occurrence of readmission due to coronary spasm was significantly lower in the -786T group than in the -786C group ($P = 0.0032$) (Fig. 3).

Risk factors for readmission due to a reattack of coronary spasm

We compared the coronary risk factors, including clinical coronary risk factors and medications, between the readmission and the non-readmission groups as is shown in Table 3. Patients in the group readmission due to a reattack of coronary spasm were significantly younger than those in the non-readmission group ($P = 0.0044$). No significant differences were seen in the other coronary risk factors or in the medications between the readmission and the non-readmission groups.

Fig. 2

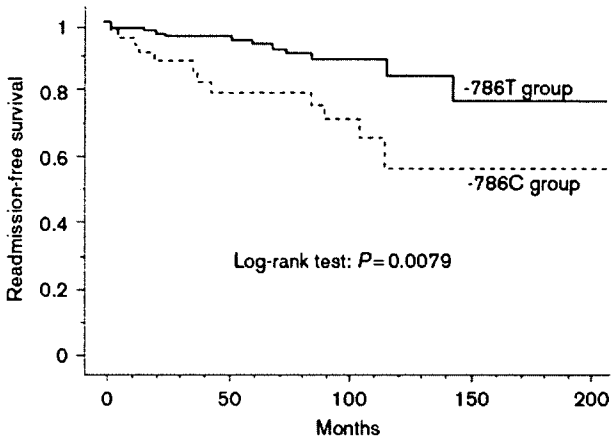

Kaplan–Meier survival curves of cumulative readmission rates in patients with coronary spasm divided into two groups according to the -786T/C polymorphism.

Fig. 3

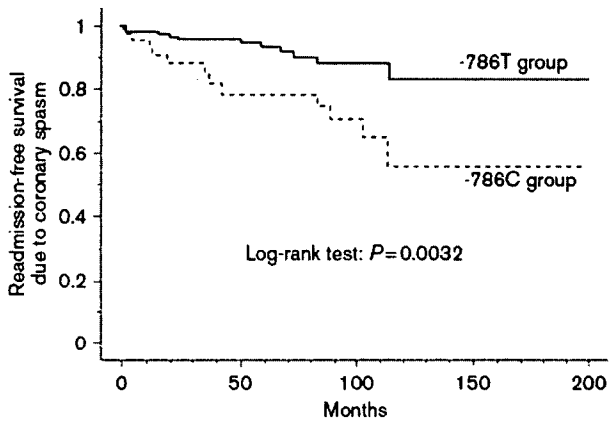

Kaplan–Meier survival curves of cumulative readmission rates due to coronary spasm in patients with coronary spasm divided into two groups according to the -786T/C polymorphism.

The rate of readmission due to a reattack of coronary spasm in the patients with T/T, C/T, and C/C genotypes were 7.6% (11/144), 22.0% (11/50), and 20.0% (1/5), respectively. The incidence of patients with the -786T/C polymorphism was significantly higher in the group of the readmission due to a reattack of coronary spasm than in the non-readmission group ($P = 0.0051$). When the additive and dominant effect of the -786C allele was analyzed, the -786C allele was significantly associated with readmission due to coronary spasm as is shown in Table 4 ($P = 0.0072$, odds ratio: 3.37 in the dominant effect).

Table 3 Clinical characteristics in readmission due to coronary spasm and non-readmission groups

	Non-readmission ($n=176$)	Readmission ($n=23$)	P value
Age (years)	63 ± 10	56 ± 12	0.0044
Men/women	86/90	12/11	NS
Hypertension	51/176 (29%)	8/23 (35%)	NS
Cigarette smoking	95/176 (54%)	14/23 (61%)	NS
Diabetes mellitus	37/176 (21%)	2/23 (9%)	NS
Hypercholesterolemia	47/176 (27%)	7/23 (30%)	NS
BMI (kg/m^2)	23 ± 3	23 ± 3	NS
Pharmacotherapy			NS
CCB	167/176 (95%)	22/23 (96%)	NS
Nitrates	20/176 (11%)	3/23 (13%)	NS
ACE-I	16/176 (9%)	2/23 (9%)	NS
Antiplatelets	22/176 (13%)	0/23 (0%)	NS
HMG-CoA Reductase inhibitor	16/176 (9%)	2/23 (9%)	NS

Values are numbers of patients or mean ± SD.
ACE-I, angiotensin-converting enzyme inhibitor; BMI, body mass index; CCB, calcium channel blocker; NS, not significant.

Table 4 Genotype frequencies of -786T/C polymorphism in the readmission due to coronary spasm and non-readmission group

	Non-readmission ($n=176$)	Readmission ($n=23$)	Odds ratio (95% CI)	P value
-786C/C genotype	4/176 (2%)	1/23 (4%)	-	-
	24%	52%		
-786C/T genotype	39/176 (22%)	11/23 (48%)		
-786T/T genotype	133/176 (76%)	11/23 (48%)	-	-
Additive	-	-	2.58 (1.26–5.21)	0.0097
Dominant	-	-	3.37 (1.39–8.20)	0.0072
Recessive	-	-	1.96 (0.21–18.29)	0.5569

Values are numbers of patients. CI, confidence interval.

Subsequently, we performed multiple logistic analysis, with forward stepwise selection for the readmission group, using all the clinical risk factors and the -786T/C polymorphism as shown in Table 5. The analysis revealed that the most predictive independent risk factor for readmission due to a reattack of coronary spasm was the -786T/C polymorphism ($P = 0.006$, relative risk = 3.590). Other classical coronary risk factors were not significant predictive factors for readmission due to coronary spasm.

CCB and readmission due to coronary spasm

We analyzed compounds and doses of CCBs, which were administered to patients with coronary spasm as shown in Table 6. The incidence of readmission due to coronary spasm was significantly higher in patients who were administered two compounds of CCBs than in patients who were administered one compound of CCBs ($P = 0.0016$).

We listed nine patients who were administered two compounds of CCBs as shown in Table 7. The incidence of the -786T/C polymorphism in the readmission and non-readmission groups were 4/4(100%) and 1/5(20.0%),

Table 5 **Multiple logistic analysis with forward stepwise selection for readmission due to coronary spasm**

Variables	β	SE	Relative risk (95% CI)	*P* value
-786T/C Polymorphism	1.278	0.461	3.590 (1.455–8.853)	0.006
Age	−0.931	0.489	0.432 (0.151–1.028)	0.057
Constant	−2.141	0.346	0.117	0.000

CI, confidence interval.

Table 6 **Compounds and doses of CCBs in the readmission due to coronary spasm and the non-readmission group**

Compounds and doses (dose per day)	Readmission (*n*=23)	Non-readmission (*n*=176)	*P* value
Diltiazem (long acting type)			
200 mg	5/23 (22%)	67/176 (38%)	NS
100 mg	3/23 (13%)	32/176 (18%)	NS
Diltiazem (short acting type)			
240 mg	0/23 (0%)	2/176 (1.2%)	NS
180 mg	1/23 (4%)	3/176 (2%)	NS
150 mg	0/23 (0%)	1/176 (0.6%)	NS
120 mg	2/23 (8%)	8/176 (5%)	NS
90 mg	0/23 (0%)	5/176 (3%)	NS
60 mg	0/23 (0%)	1/176 (0.6%)	NS
Nisoldipine			
20 mg	1/23 (4%)	3/176 (1.7%)	NS
15 mg	1/23 (4%)	0/176 (0%)	NS
10 mg	4/23 (17%)	21/176 (12%)	NS
5 mg	0/23 (0%)	6/176 (3%)	NS
Nifedipine			
80 mg	1/23 (4%)	1/176 (0.6%)	NS
60 mg	0/23 (0%)	1/176 (0.6%)	NS
40 mg	0/23 (0%)	2/176 (1.2%)	NS
20 mg	0/23 (0%)	4/176 (2.2%)	NS
Benidipine			
8 mg	0/23 (0%)	2/176 (1.2%)	NS
Amlodipine			
5 mg	0/23 (0%)	2/176 (1%)	NS
2.5 mg	0/23 (0%)	1/176 (0.6%)	NS
Two CCB compounds	4/23 (17%)	5/176 (3%)	0.0016

Values are numbers of patients.
CCB, calcium channel blocker; NS, not significant.

respectively. In the patients with two compounds of CCBs, the incidence of the -786T/C polymorphism was significantly higher in the readmission group than in the non-readmission group ($P = 0.0164$).

Discussion

Prognosis and readmission in patients with coronary spasm

As with others, we have previously reported that the prognosis for coronary-spasm patients without coronary stenosis was relatively good [4,5]. We have also reported that the intake of CCB, multivessel spasm, and the severity of coronary artery disease are all significant independent predictors of survival for patients without myocardial infarction [4]. In this study population, patients with significant organic stenosis were excluded. All the study patients took CCB and/or nitrate during the follow-up period; there were no cardiac deaths during this period in this study. This result is in accordance with many previous studies. On the other hand, there were 25 study patients (12%) who were readmitted owing to coronary events: 92% of the readmissions were due to a reattack of coronary spasm. Sueda *et al.* [6] recently suggested that 42% of the patients with pure coronary spastic angina had a reattack of coronary spastic angina during the administration of CCB. The outcomes in Sueda's coronary-spasm patients are in general agreement with our results.

Table 7 **Characteristics of patients who were administered CCB two compounds**

Patient no.	Age	Sex	-786T/C genotype	Hypertension	Cigarette smoking	Diabetes mellitus	Hypercholesterolemia
Non-readmission							
1	53	M	T/T	−	+	−	−
2	64	M	T/T	+	+	−	−
3	66	F	T/T	+	+	−	−
4	68	M	T/T	−	+	−	−
5	74	F	C/T	−	−	−	−
Readmission							
6	40	M	C/T	−	+	−	+
7	66	M	C/T	+	−	−	+
8	67	M	C/C	−	+	−	−
9	76	F	C/T	−	−	−	−

F, female; M, male.

In this study, the readmitted patients were significantly younger than the non-readmitted patients. We therefore suggest that the disease-activity level of coronary spastic angina is higher in younger patients than in the older ones. Younger patients may be more susceptible to getting coronary spastic angina as a result of coronary spasm. Further study is needed to clarify whether there is a significant difference in the disease activity level of coronary spasm between younger and older patients.

Readmission and the endothelial nitric oxide synthase polymorphism

The incidence of readmission was significantly higher in the -786C group than in the -786T group. The -786T/C polymorphism was significantly associated with readmission due to coronary arterial events. Multiple logistic regression analysis revealed that the -786C allele was the most predictive independent risk factor for readmission in patients with coronary spasm. It is possible that the -786T/C polymorphism reduces eNOS gene expression in the coronary arterial endothelial cells, and thereby predisposes the patients to recurrent coronary spasm even if the patients have taken CCB.

Readmission due to acute myocardial infarction

In this study, there was a patient who had acute myocardial infarction during the follow-up period. Significantly, he had the -786C/C genotype. As this patient had no coronary stenosis, myocardial infarction was most probably caused by coronary spasm. Although this patient had taken CCB, he had an incident of acute myocardial infarction. Thus, it is suggested that the -786T/C polymorphism predisposes patients to have myocardial infarction due to coronary spasm, even while being administered CCB.